



Introduction to CLIC

Walter Wuensch
KVI, Groningen
25 March 2011



Outline



- The linear collider landscape
- The CLIC machine
- High-gradient rf development



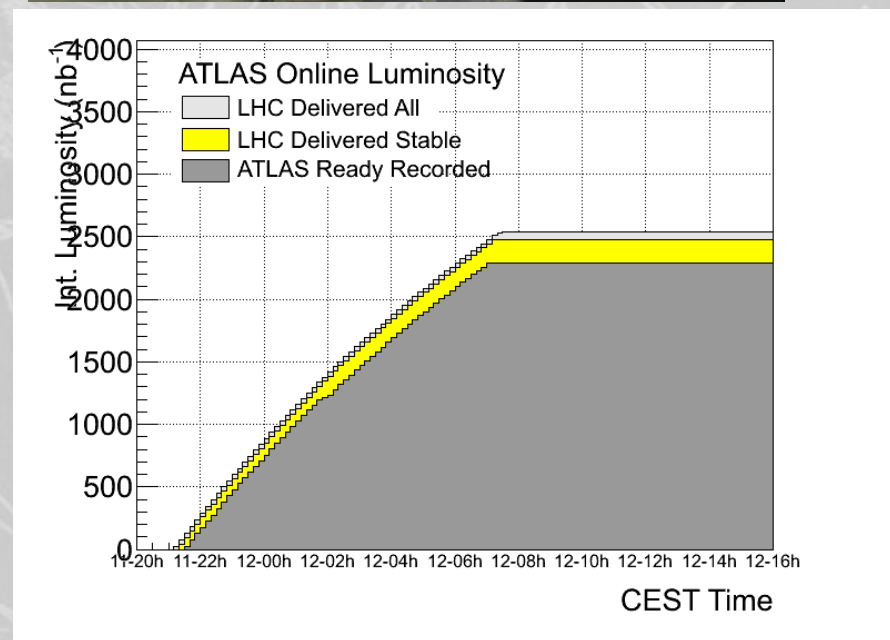
State-of-the-art in TeV facilities

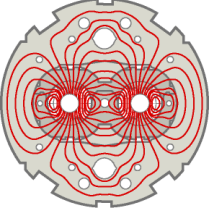


The LHC at CERN, has just started its second year of operation at a 7 TeV center of mass energy with proton-proton collisions.

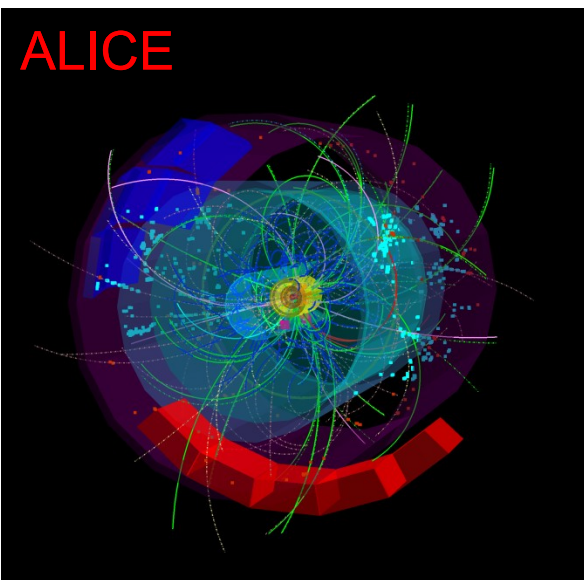
The energy will be increased to the design specification of 14 TeV in the coming years.

Upgrades in luminosity and/or energy are already being discussed.

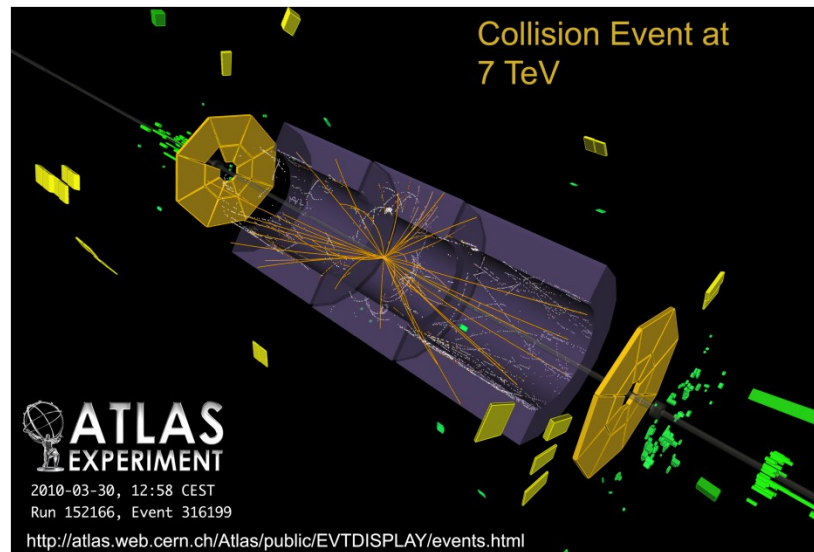




LHC: First collisions at 7 TeV on 30 March 2010



ALICE



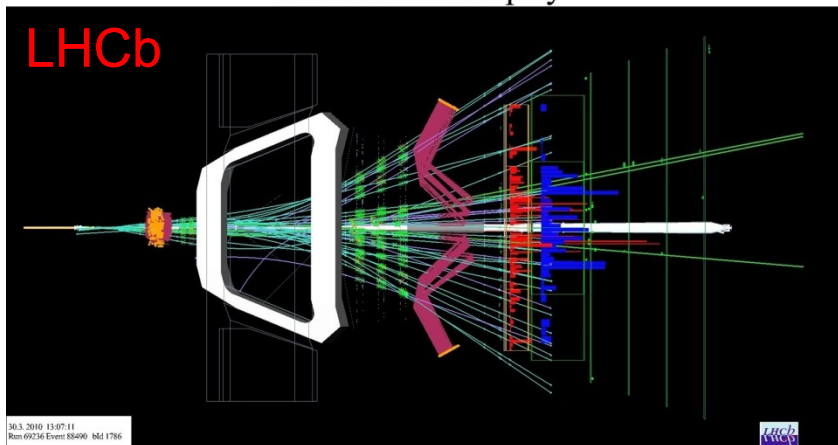
Collision Event at 7 TeV

ATLAS EXPERIMENT

2010-03-30, 12:58 CEST
Run 152166, Event 316199

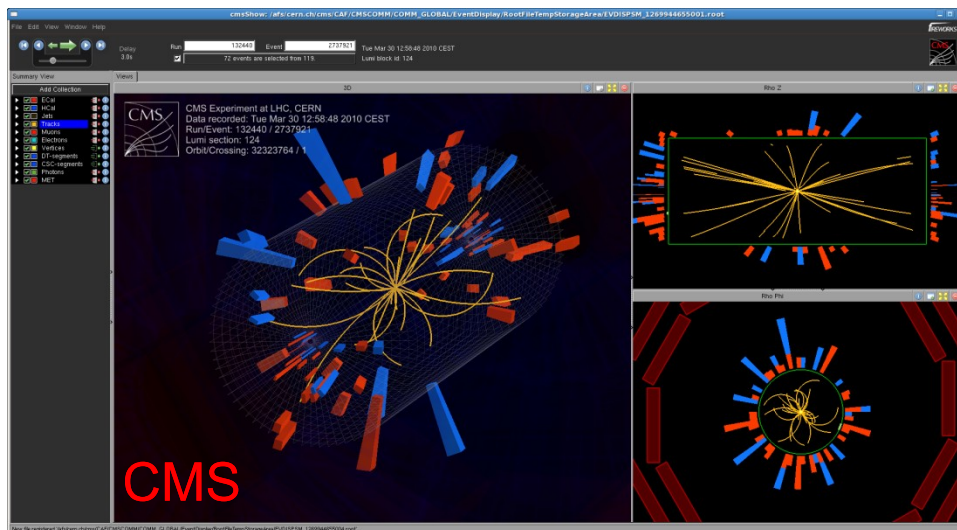
<http://atlas.web.cern.ch/Atlas/public/EVTDISPLAY/events.html>

LHCb Event Display



LHCb

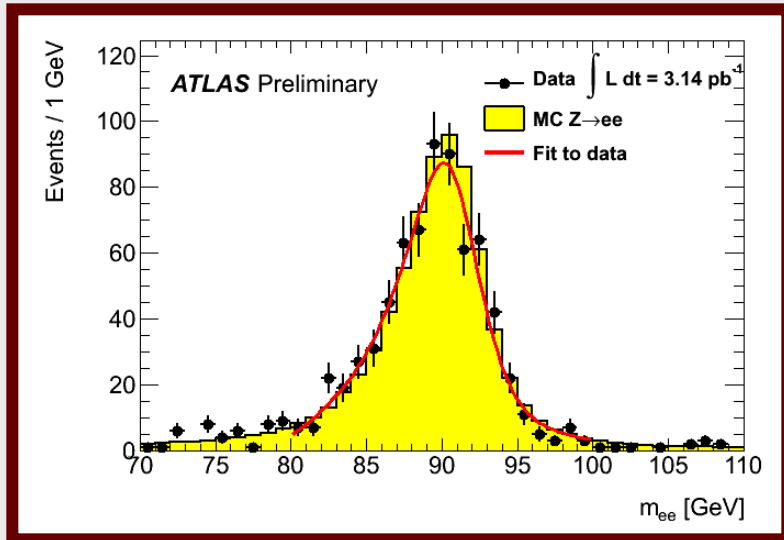
30.3.2010 13:07:11
Run 60256 Event 33490 NSL 1756



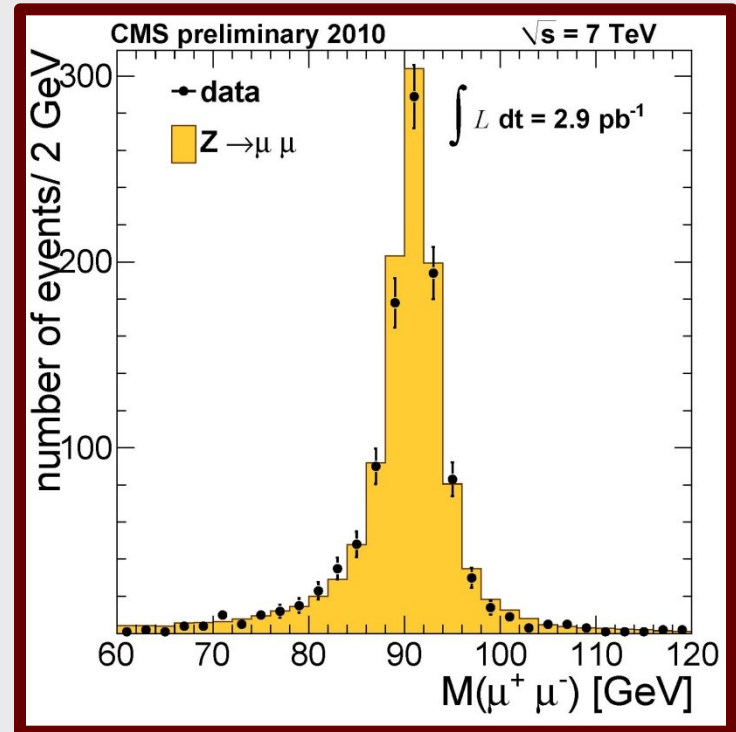
CMS

What's new since Beijing

- Experiments are performing very well

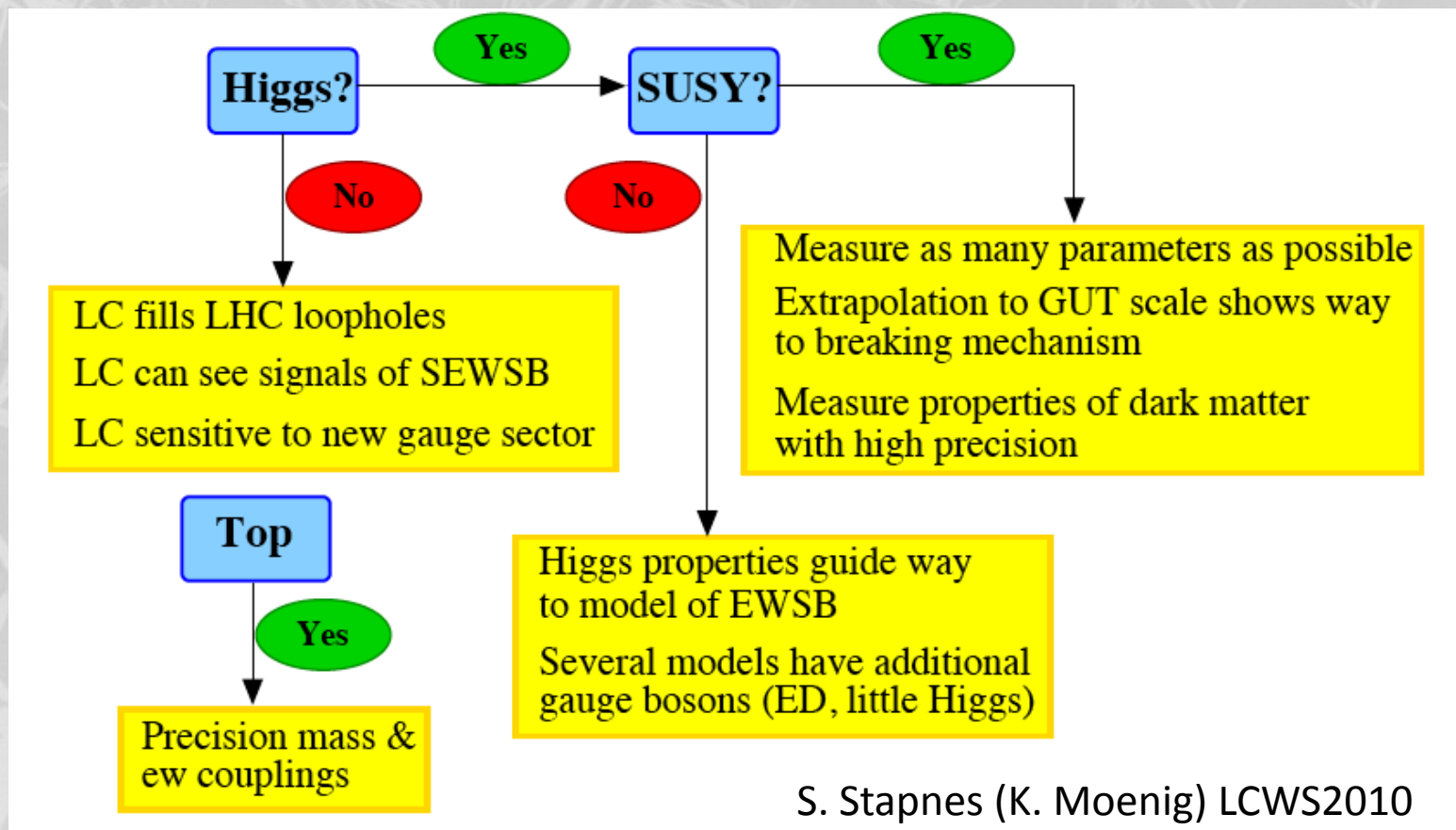


EM energy scale known to 1-3%
Resolution approaching MC value



Muon scale known to $\sim 1\%$ (or better) in Z-region
Resolution approaching MC value

Many new physics discoveries are hoped for from the LHC - Higgs, super symmetry, dark matter. Many of these new particles could then be better studied in detail using the simpler experimental environment of **lepton** collisions.





e^+e^- linear colliders



Electron-positron linear colliders operating in the range of 0.5 to 3 TeV to complement the LHC are under active study.

The energy of a future linear collider is expected to be determined more precisely from the physics results produced by the LHC in the next two years or so.

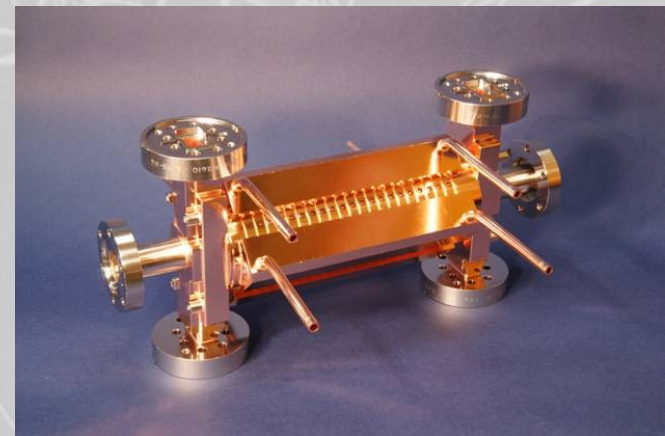
(The lower energy compared to the LHC is that only the energy of individual constituent quarks and gluons of the protons, six in total, that actually contribute to the relevant interaction.)

ILC and CLIC

There are two main approaches currently formalized as projects: ILC and CLIC

- The ILC is superconducting with a gradient of 31.5 MV/m
- CLIC is normal conducting with an accelerating gradient of 100 MV/m.

		CLIC	CLIC	ILC
E_{cms}	[TeV]	0.5	3.0	0.5
f_{rep}	[Hz]	50	50	5
f_{RF}	[GHz]	12	12	1.3
G_{RF}	[MV/m]	80	100	31.5
n_b		354	312	2625
Δt	[ns]	0.5	0.5	369
N	[10^9]	6.8	3.7	20
σ_x	[nm]	202	40	655
σ_y	[nm]	2.26	1	5.7
ϵ_x	[μm]	2.4	0.66	10
ϵ_y	[nm]	25	20	40
\mathcal{L}_{total}	[$10^{34}\text{cm}^{-2}\text{s}^{-1}$]	2.3	5.9	2.0
$\mathcal{L}_{0.01}$	[$10^{34}\text{cm}^{-2}\text{s}^{-1}$]	1.4	2.0	1.45



The early days of multi-TeV linear colliders

EUROPEAN ORGANIZATION FOR NUCLEAR RESEARCH

CERN-LEP-RF/86-06

and

CLIC NOTE 13
13.2.86

A TWO-STAGE RF LINAC COLLIDER
USING A SUPERCONDUCTING DRIVE LINAC

M. Schnell

Abstract

The efficiency from RF input to beam power of a normal conducting travelling-wave linac can be raised above 5% albeit at the price of a very short pulse and an appreciable but probably correctible energy spread. Compensated multibunch operation may yield 30% efficiency but higher order wakefield problems have to be solved and a suitable final focus system must be found. The worst remaining problem seems to be the economic and efficient generation of peak RF power. The solution proposed here consists of a limited number of MW UHF klystrons, a superconducting UHF drive linac and a tightly bunched drive beam of several GeV average energy, transferring energy from the superconducting linac to the main linac via short sections of transfer structures. The power balance of this scheme is analysed and it is found that overall efficiency can be very high. Very dense drive bunches are required. Present-day performance of superconducting cavities is already sufficient to make the scheme viable at main linac accelerating gradients approaching 100 MV/m.

Geneva, Switzerland
February 1986

APR 7 1986
ISIS LIBRARY

CLIC Note 38
(May, 1987)

ORGANISATION EUROPÉENNE POUR LA RECHERCHE NUCLÉAIRE
CERN EUROPEAN ORGANIZATION FOR NUCLEAR RESEARCH

REPORT FROM THE ADVISORY PANEL ON THE PROSPECTS
FOR e^+e^- LINEAR COLLIDERS IN THE TeV RANGE

GENEVA
1987

The years of many linear collider studies

MPI-PhE/93-14
ECFA 93-154
Vol. I
June 1993

LC92

ECFA WORKSHOP ON e^+e^- LINEAR COLLIDERS



25 July - 2 August 1992

PROCEEDINGS
VOL. I

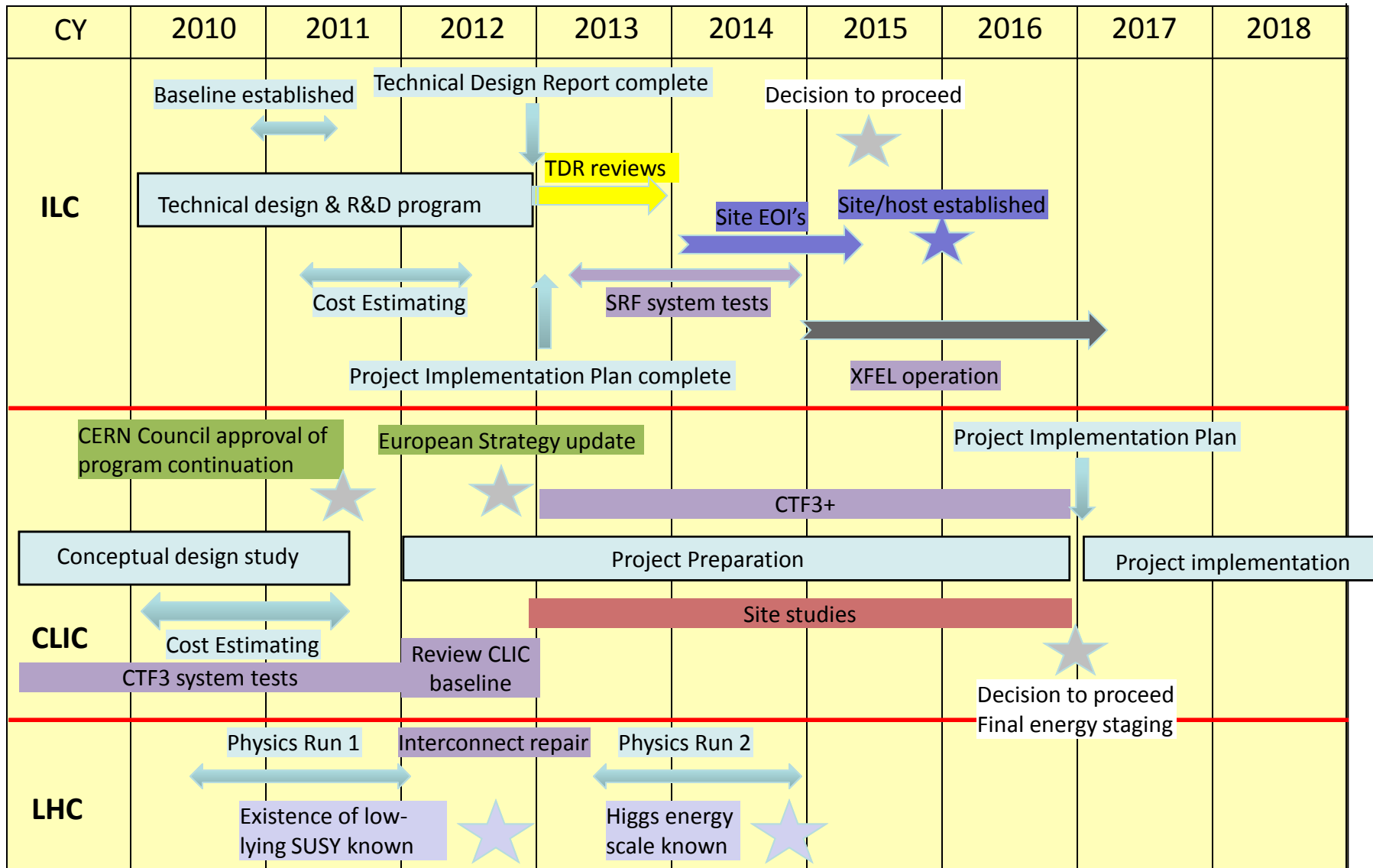
EDITOR: Ron Seidler

TABLE OF CONTENTS

Volume I. Introductory Session

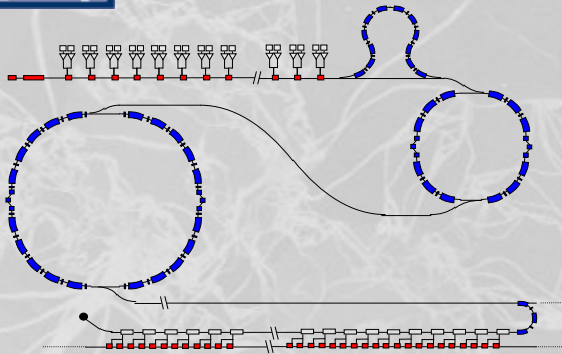
Forward	v
List of Attendees	vii
Opening Address	
Guy Coignet	1
Physics with Linear Colliders	
Peter Zerwas	11
SLC	
John Seeman	93
DLC	
Thomas Weiland	121
NLC	
Ronald Ruth	156
JLC	
Koji Takata	207
TESLA	
Maury Tigner	227
VLEPP	
Vladimir Balakin	243
CLIC	
Wolfgang Schnell	267
FFTB	
David Burke	283
Appendices	
Appendix A. Addresses of Attendees	a1
Appendix B. Bit of the Action	a15

CLIC & ILC roadmaps

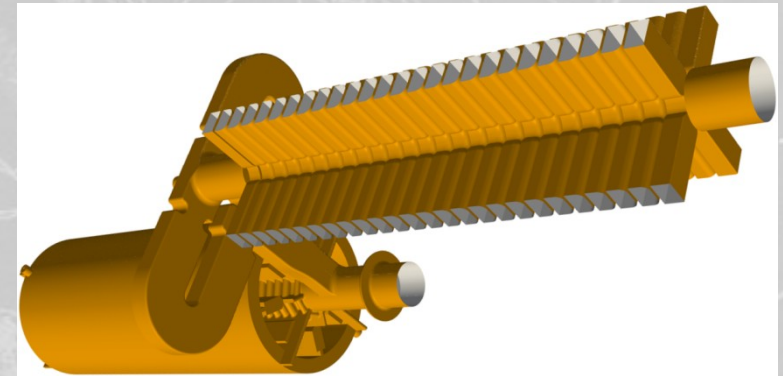




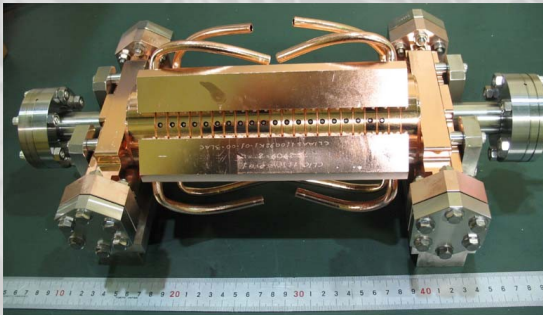
The CLIC machine



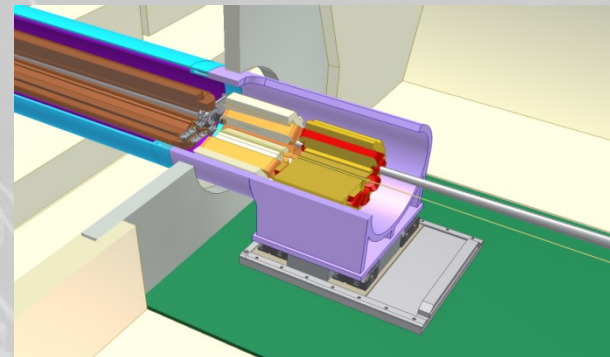
Beam-based pulse compression



Two-beam acceleration



High-gradient rf acceleration



Low emittance beams
(not covered today)



Beam-based pulse compression



The total peak 12 GHz power required to feed the whole CLIC linac for 3 TeV center of mass energy and 100 MV/m acceleration is around of 8 TW with a total rf pulse energy of around 8 MJ.

Consequently CLIC, like most linacs, is a pulsed machine. The CLIC duty cycle is very low, around 10^{-5} .

CLIC has a beam-based scheme for storing energy and then compressing it, a logical approach for a laboratory specialized in particle beams.



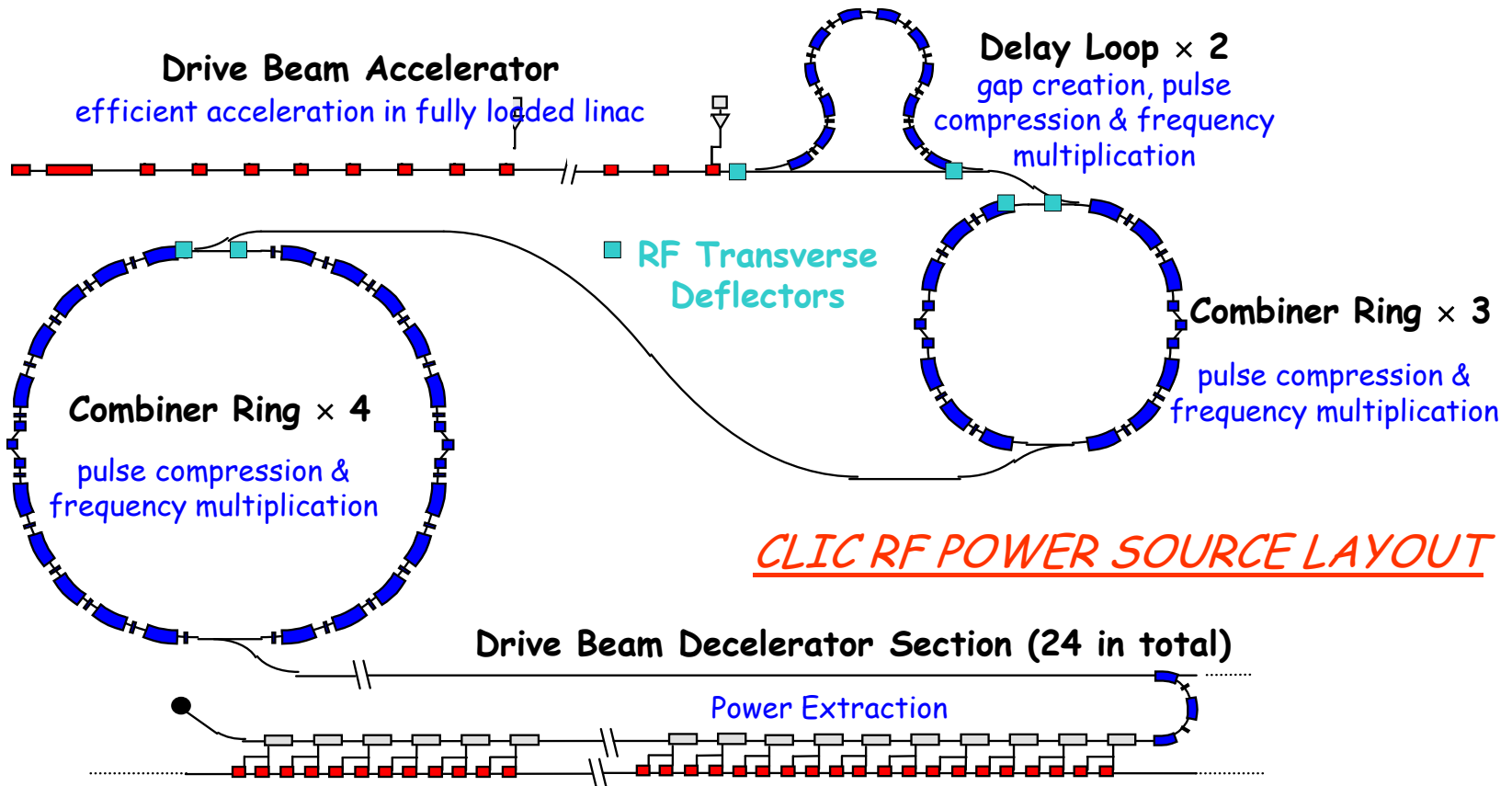
Beam-based pulse compression



Step 1: Energy transferred from mains to 100 A, 2.4 GeV and 140 μ s drive beam via fully loaded 1 GHz linac fed by long pulse klystron/modulator. Factor 143.

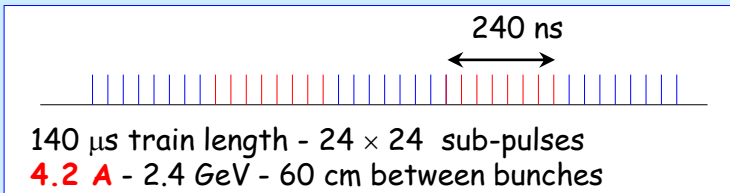
Step 2: Beam compression delaying loops and rings. This is an active pulse compressor based on rf deflection. Factor 24.

Step 3: Counter-flowing drive and main beam. Factor 24.

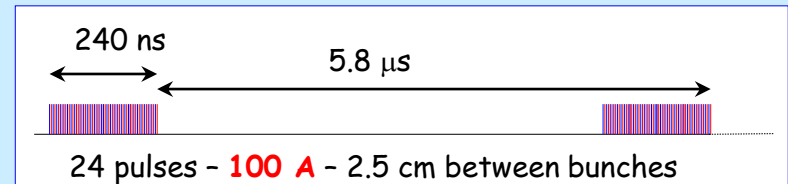


CLIC RF POWER SOURCE LAYOUT

Drive beam time structure - initial



Drive beam time structure - final



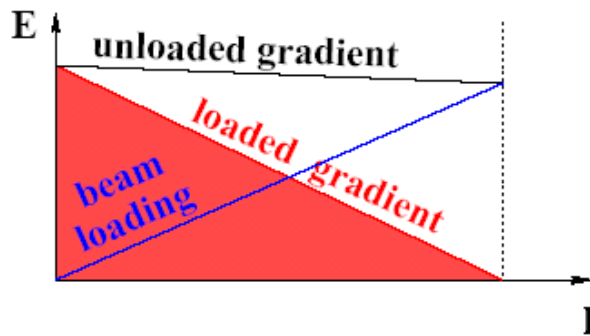
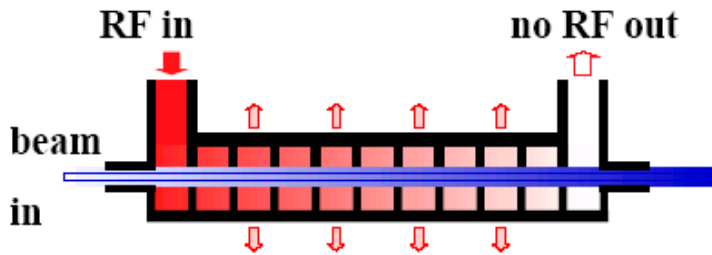
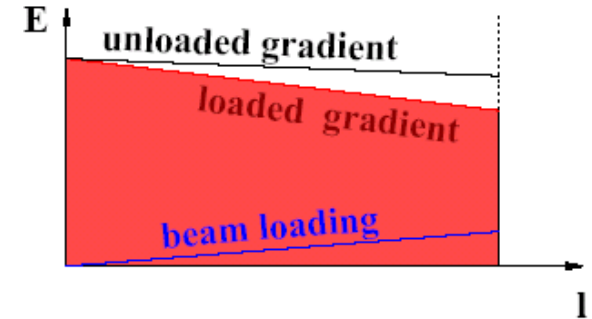


Let's follow the power

- **efficient** power transfer from RF to the beam needed

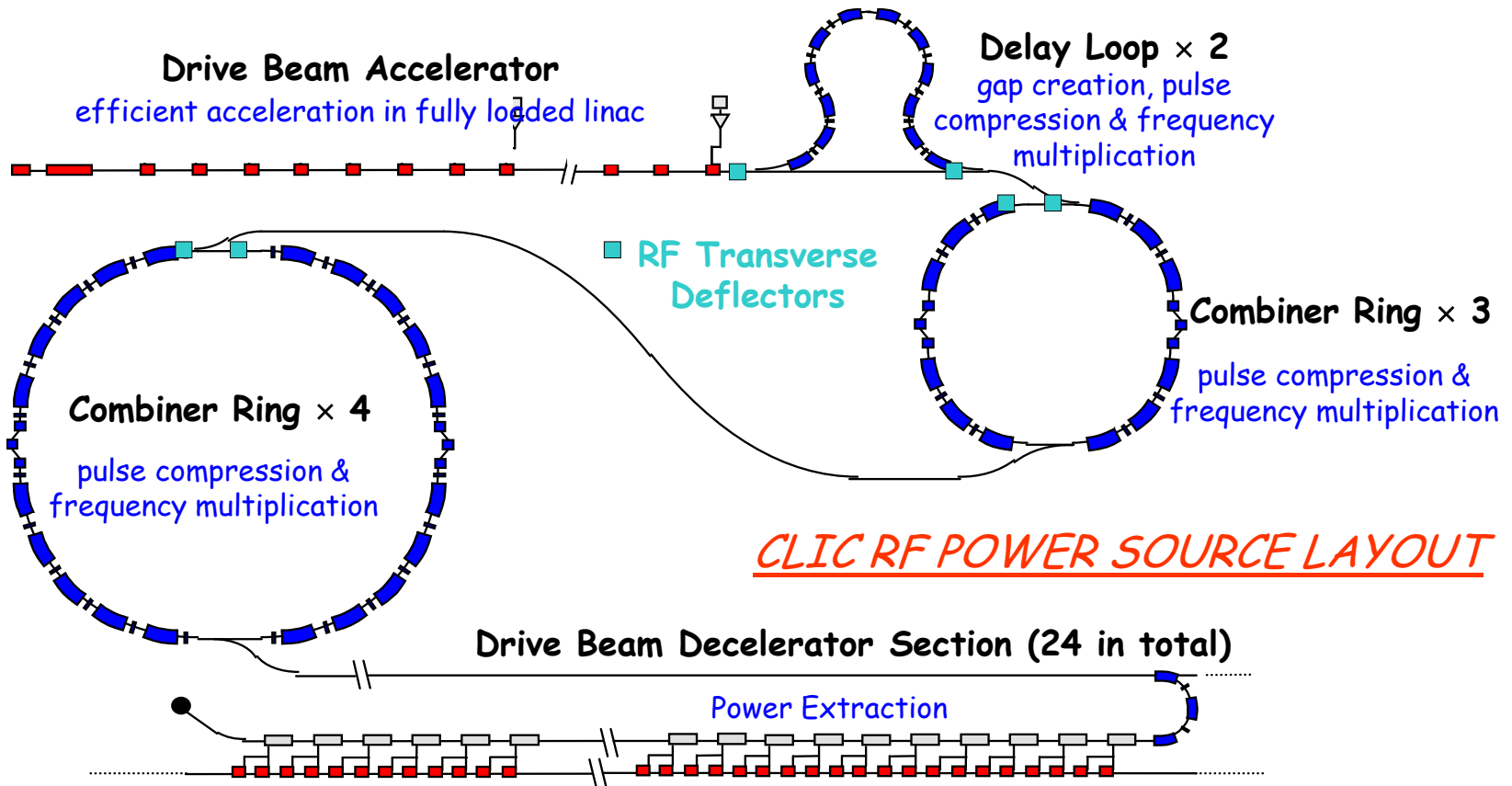
“Standard” situation:

- **small** beam loading
- power at structure exit lost in load

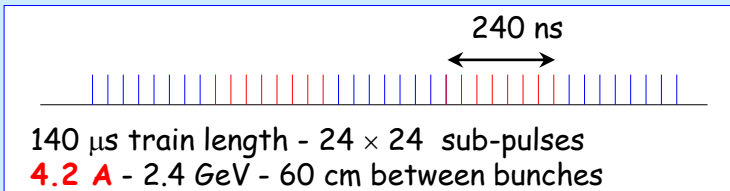


“Efficient” situation:

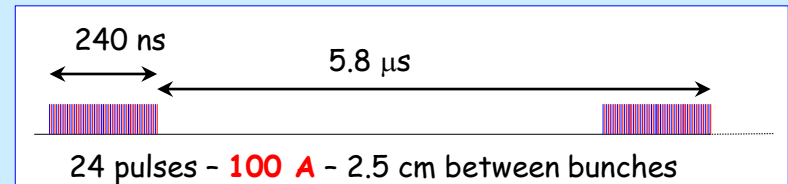
- high beam current
- **high** beam loading
- no power flows into load
- $V_{ACC} \approx 1/2 V_{unloaded}$



Drive beam time structure - initial



Drive beam time structure - final





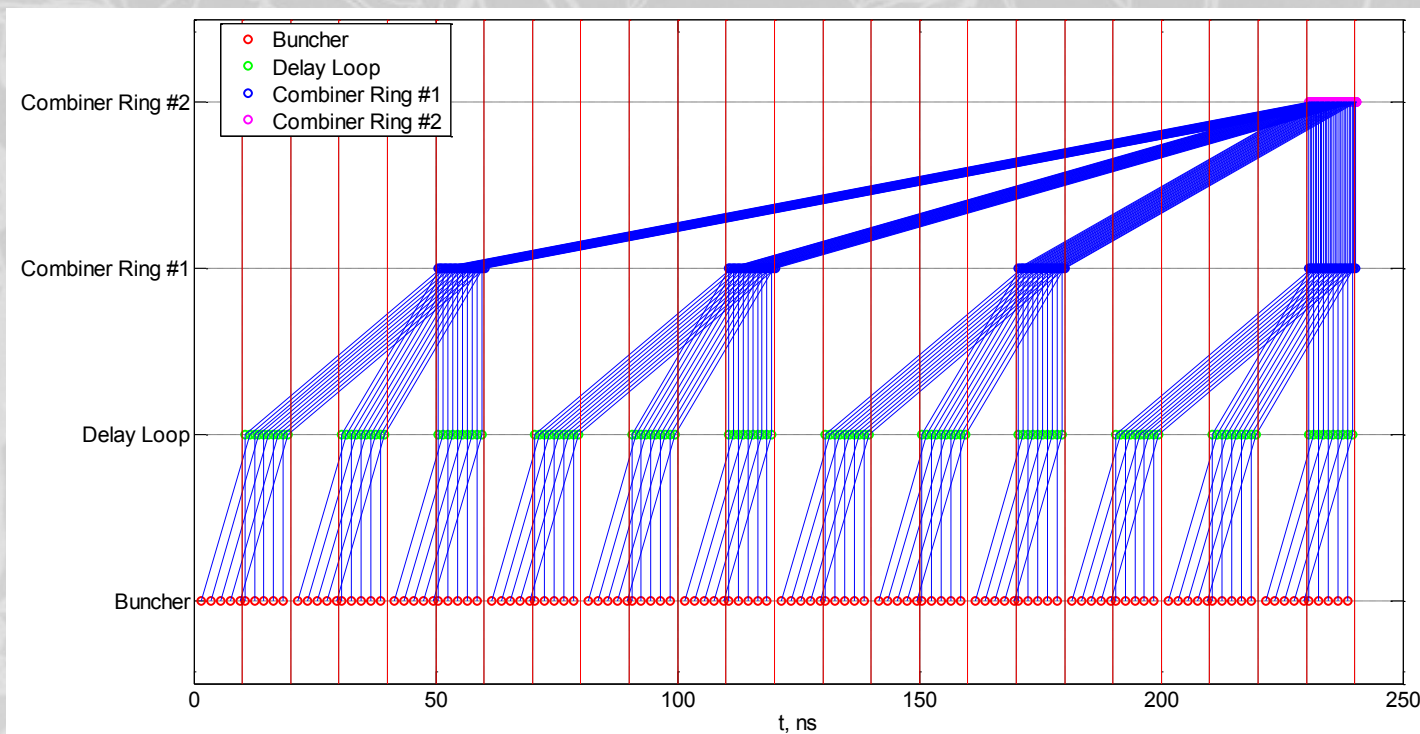
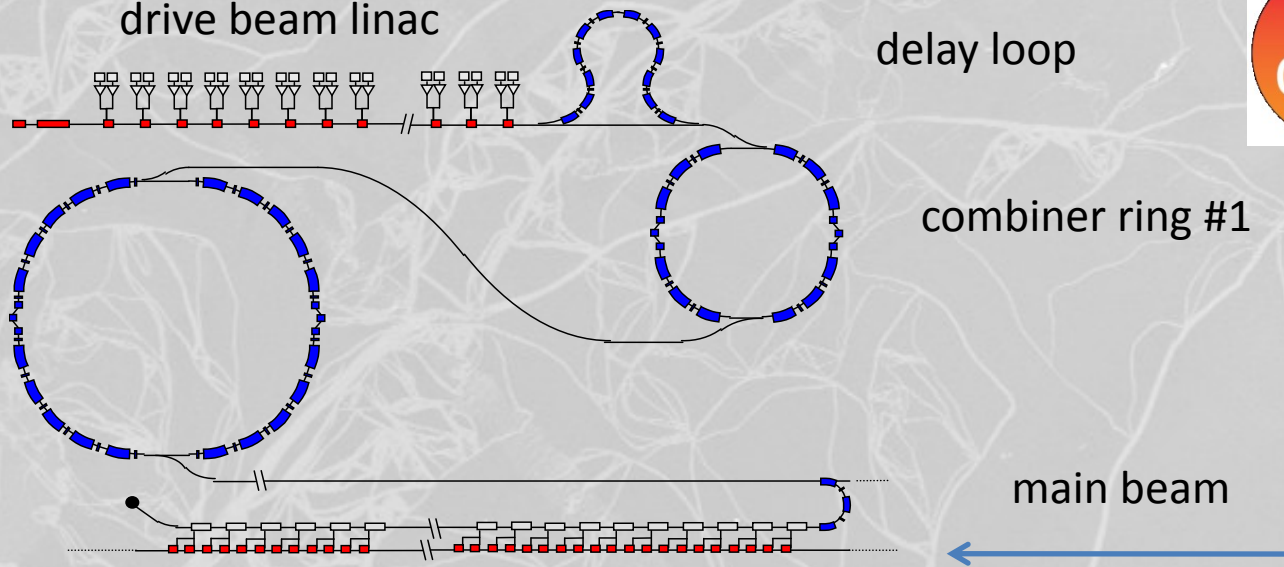
drive beam linac

delay loop

combiner ring #1

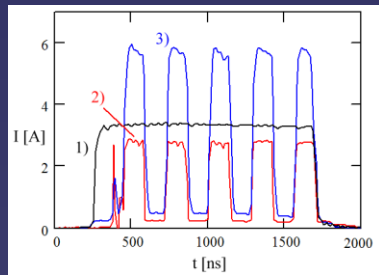
combiner ring #2

main beam



CTF3 completed, operating 10 months/year, under commissioning: Drive Beam Generation demonstrated

Fully loaded acceleration
RF to beam transfer:
95.3 % measured



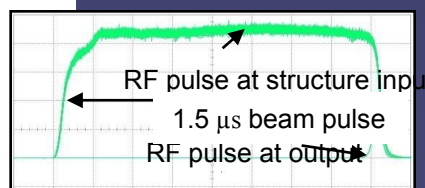
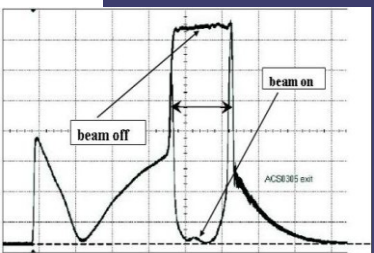
7 A @ 3 GHz

DELAY LOOP

COMBINER RING

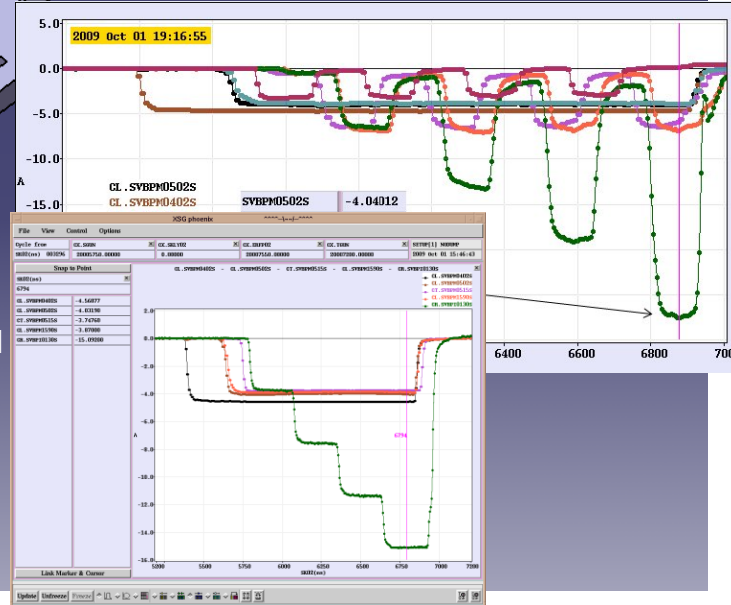
27 A @ 12 GHz

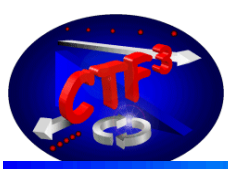
4 A - 1.2 μ s
120 Mev @ 1.5 GHz



DRIVE BEAM LINAC

CLEX
CLIC Experimental Area

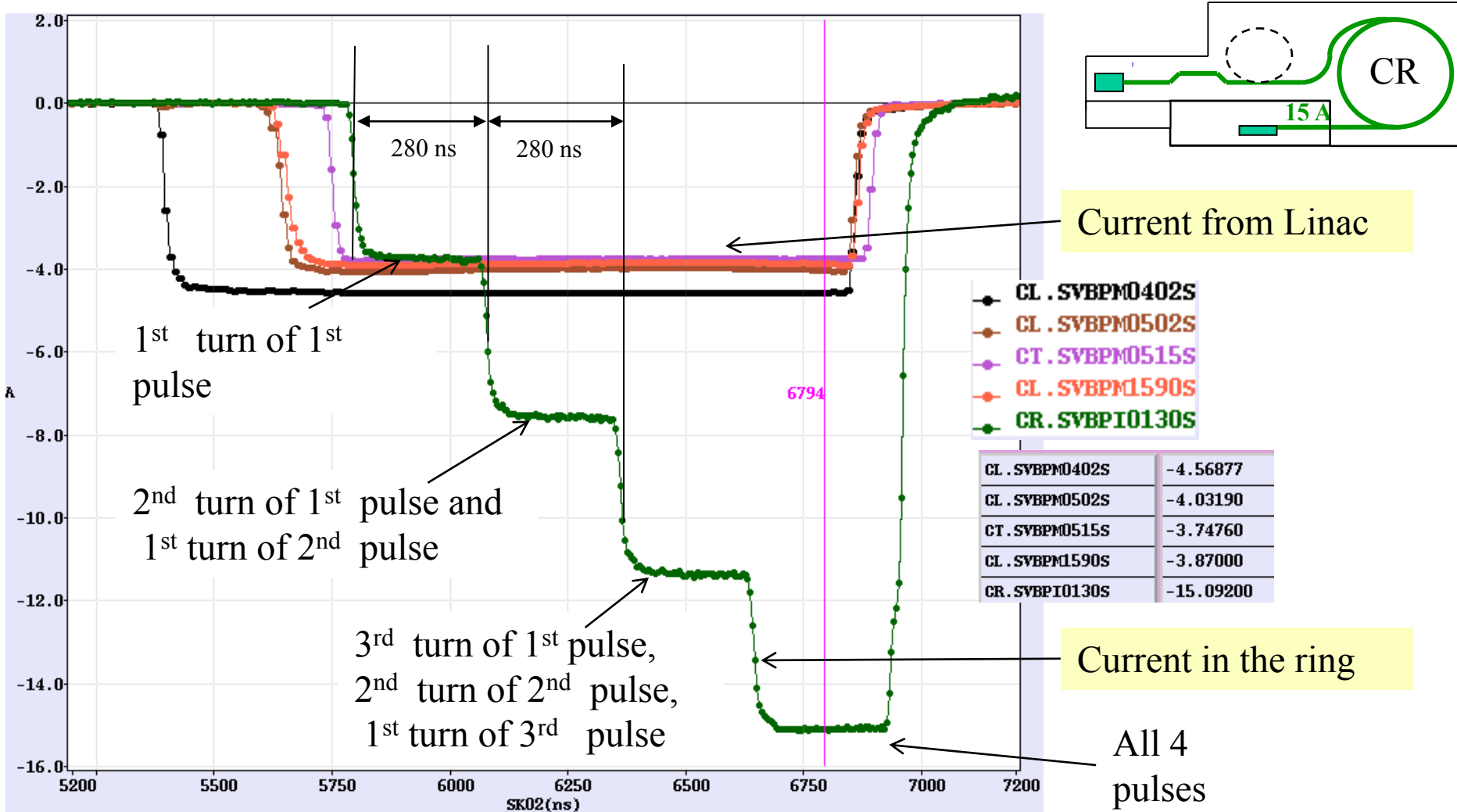


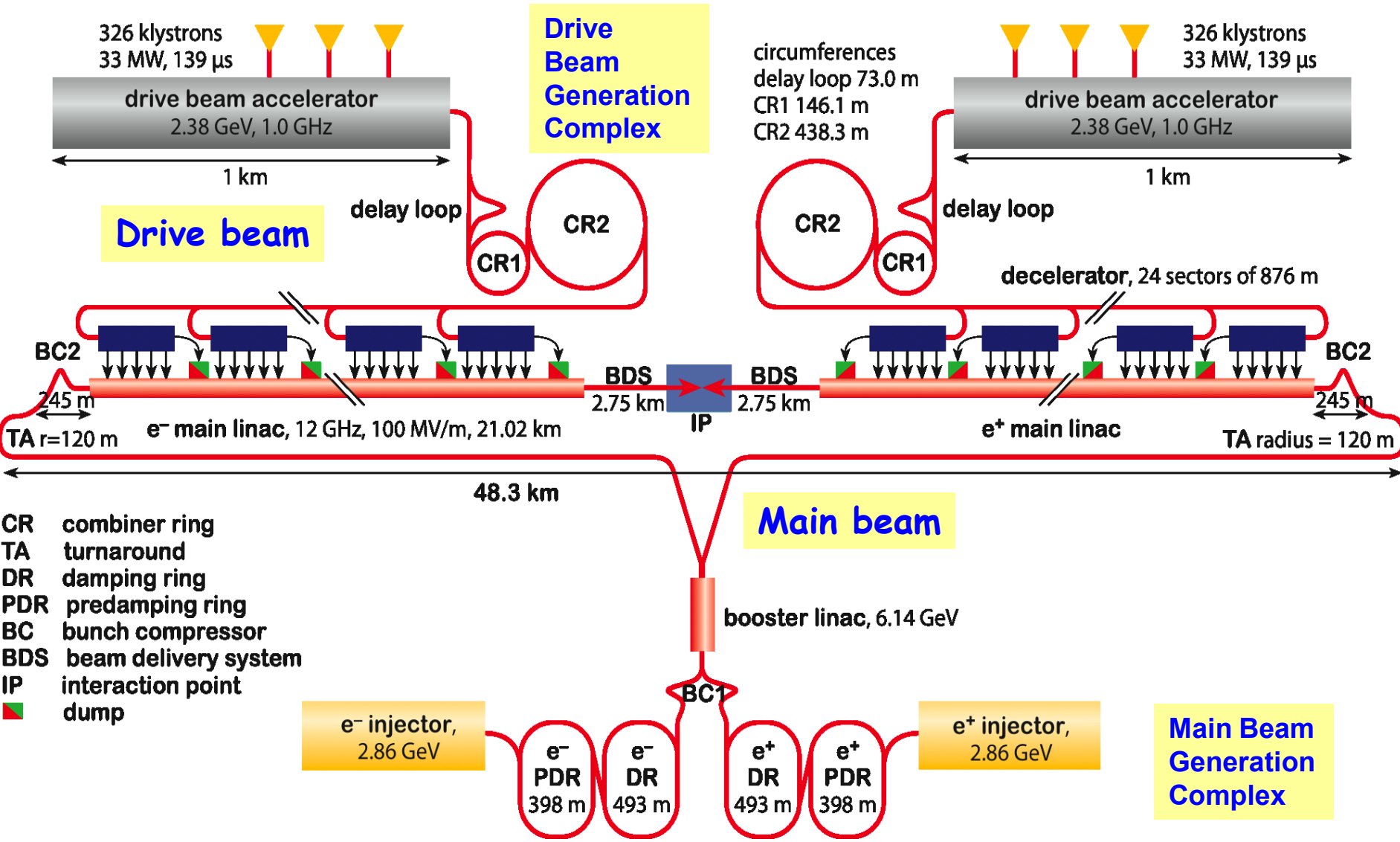


Combiner ring status



factor 4 combination achieved with 15 A, 280 ns (without Delay Loop)







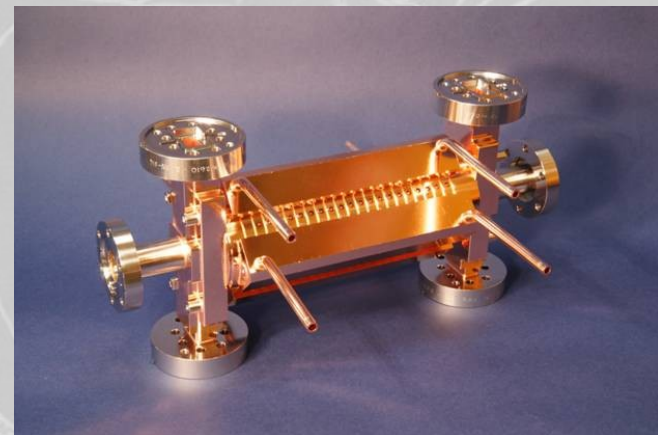
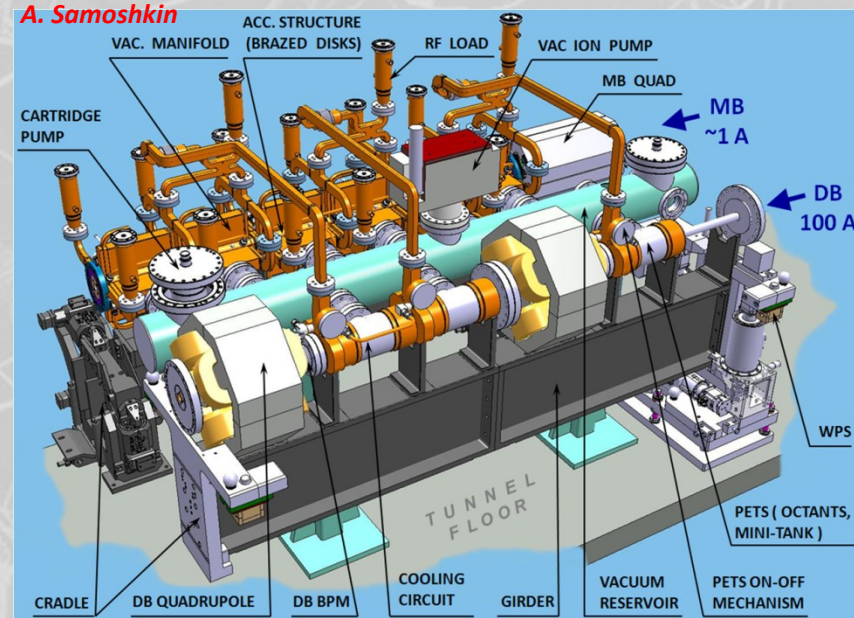
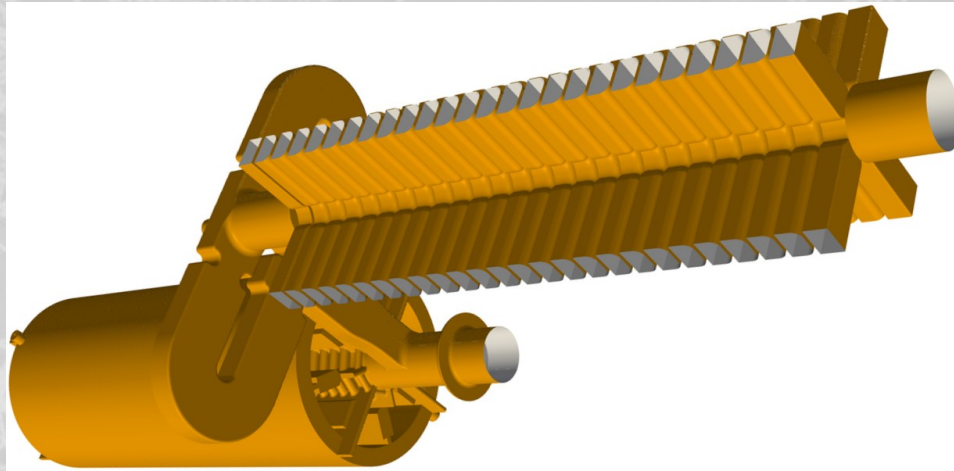
Two-beam acceleration



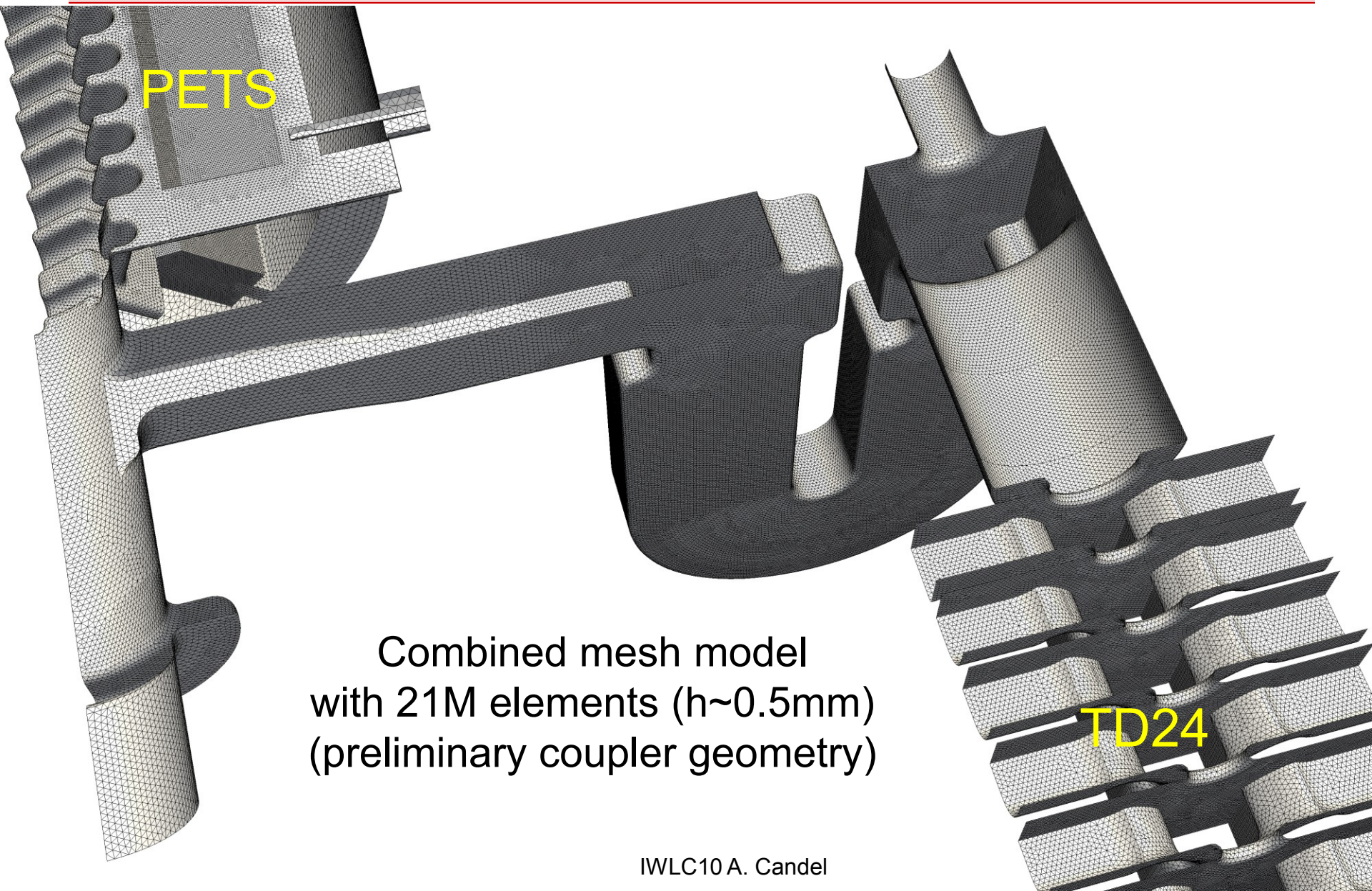
The next trick is transfer the kinetic energy of the 100 A drive beam to the 1A main beam via a two-beam “rf transformer”

Here the so-called PETS (Power extraction and transfer structure) decelerate the drive beam with a gradient of -5.7 V/m to produce 135 MW of power in order to feed two accelerating structures with a gradient of 100 MV/m.

Elements of CLIC two-beam



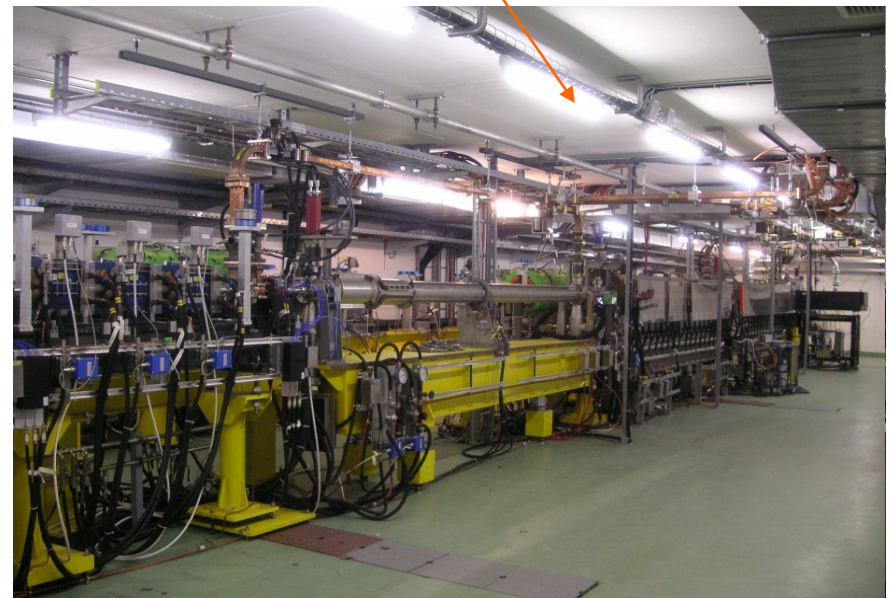
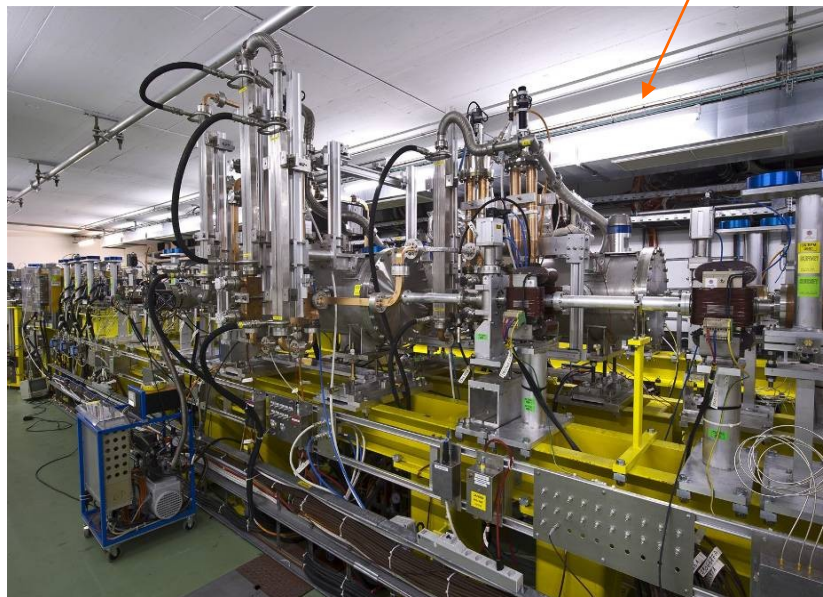
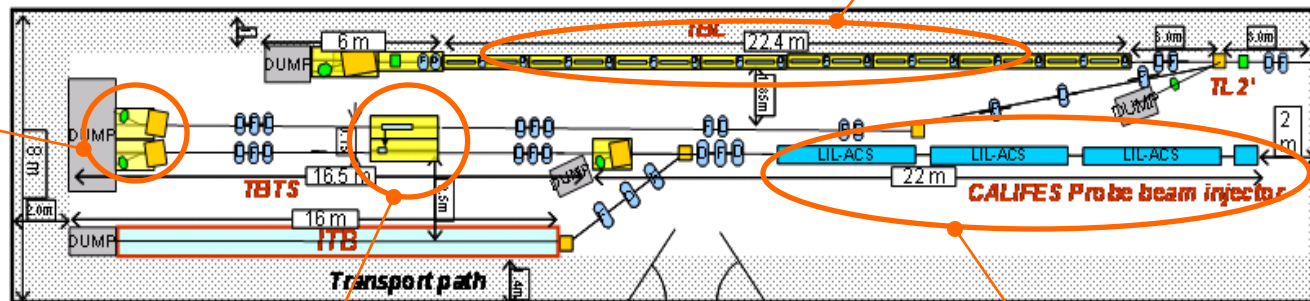
T3P: Wakefield Coupling PETS \leftrightarrow TD24



Combined mesh model
with 21M elements ($h \sim 0.5\text{mm}$)
(preliminary coupler geometry)



TBTS is the test area in CLEX, where feasibility of the CLIC two beam acceleration scheme is...already demonstrated (not yet at a nominal 100 MV/m accelerating gradient).

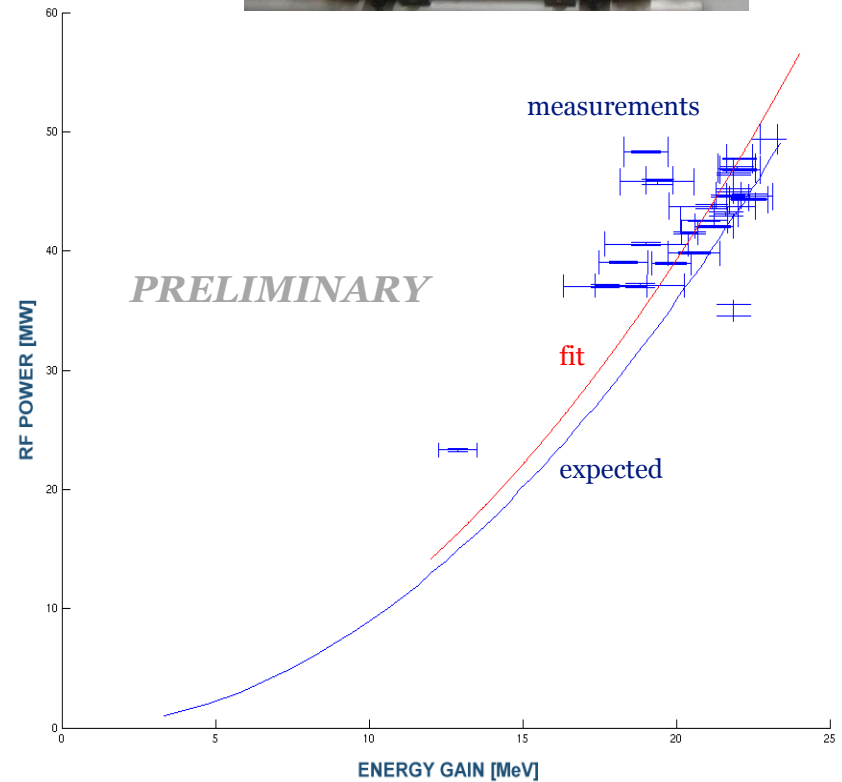
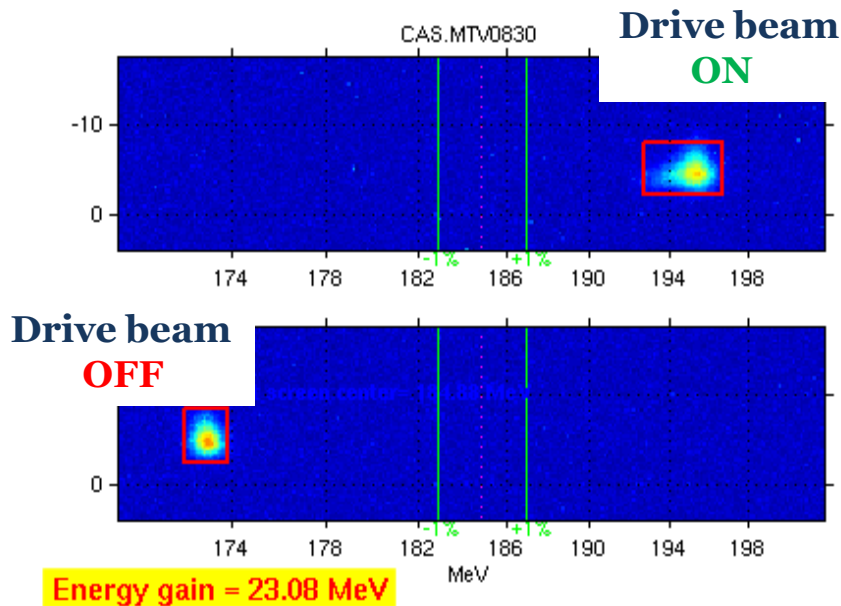
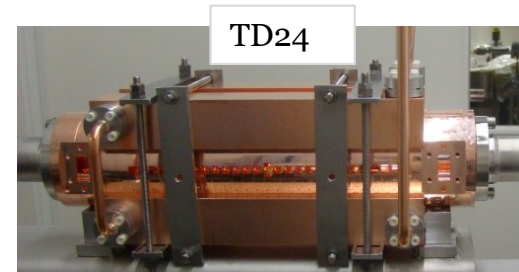




Two-Beam Acceleration demonstration in CTF3 Two-Beam Test Stand

Maximum probe beam acceleration of **23 MeV** measured

⇒ Corresponding to a gradient of **106 MV/m**





Development of high-power and high-gradient
rf structures

because

The energy reach of a linear collider is largely
determined by the accelerating gradient.



We follow the power again



PETS – specifications

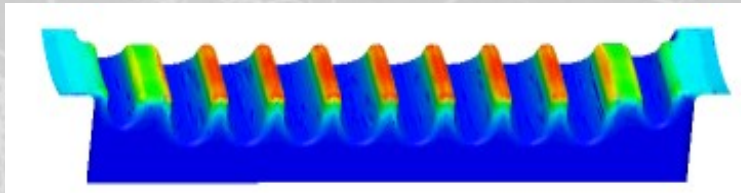


High-power:

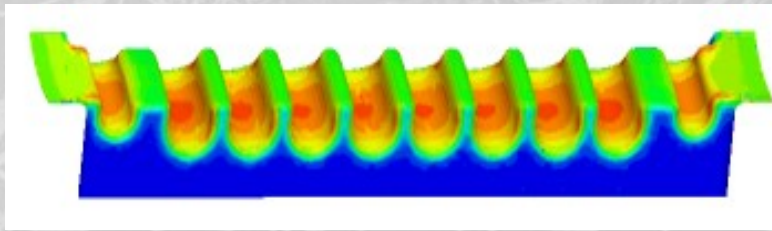
1. 135 MW output power
2. 170 (flat top)/240 (full) ns pulse length
3. $<2 \times 10^{-7}$ 1/pulse/m breakdown rate

Beam dynamics:

1. Fundamental mode: gives 23 mm diameter aperture which corresponds to $a/\lambda=0.46$ and $v_g/c=0.49$ to give 2.2 k Ω /m, longitudinal impedance
2. Single bunch transverse wake: < 8 V/pC/mm/m
3. Long-range transverse wakefield with effective suppression of main HOMs by $Q_n(1-\beta_n)<8$ each



Surface electric field



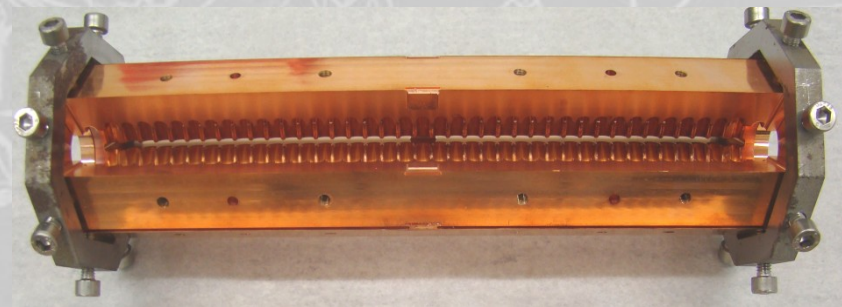
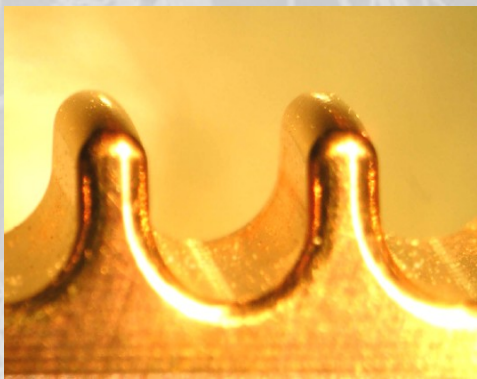
Surface magnetic field

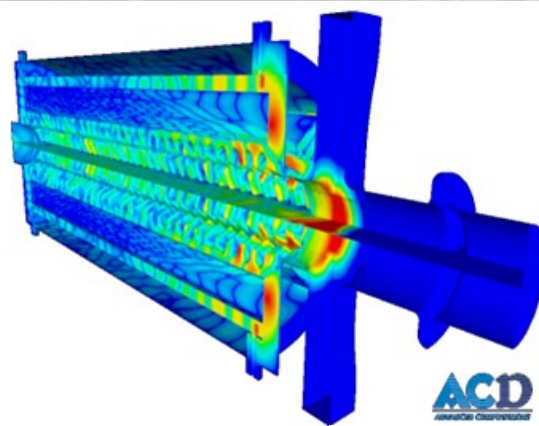
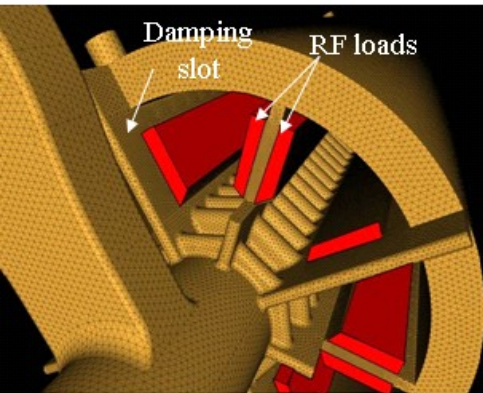
Beam-driven structure so power rises quadratically with current and length,

- 135 MW for 100 A beam
- 213 mm active length

Maximum fields at output with values,

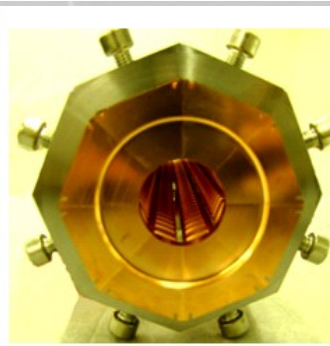
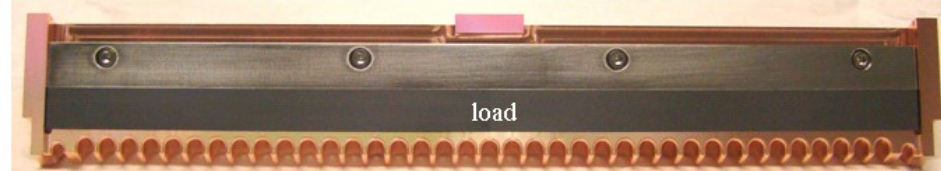
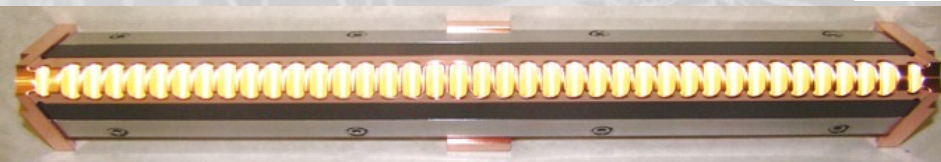
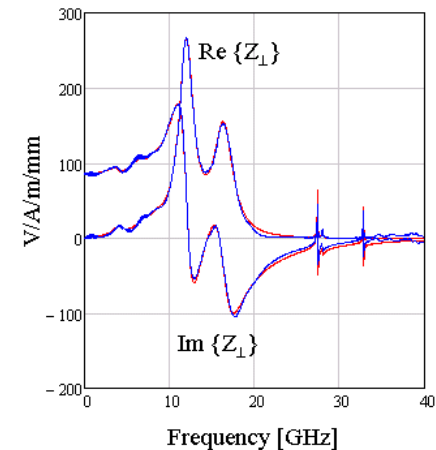
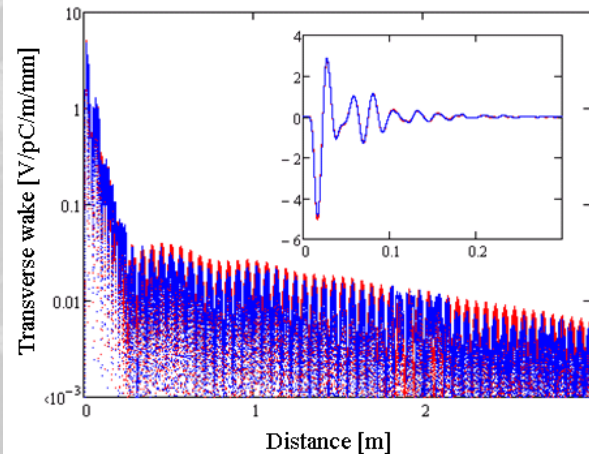
- $E_{\text{surf}}=56$ MV/m
- $\Delta T=1.8$ ($H_{\text{surf}}=0.08$ MA/m)
- $S_c=1.2$ MW/mm²





ACE3P analysis of HOM properties

GdfidL and ACE3P benchmarking with analysis of PETS HOM properties



PETS for high-power testing with SiC absorbers installed.

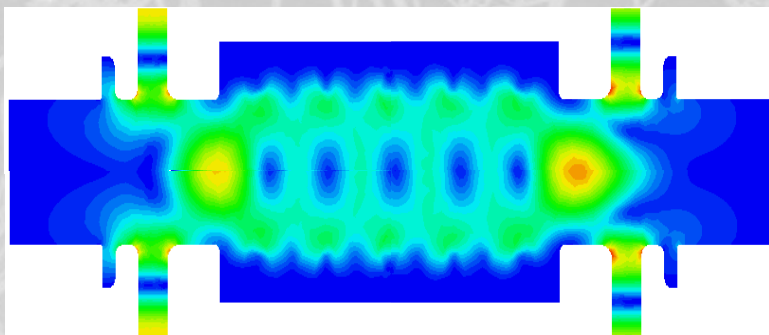
To high-power test the PETS in nominal conditions would require a 100 A driving beam.

“Waveguide” test with klystron/pulse compressor

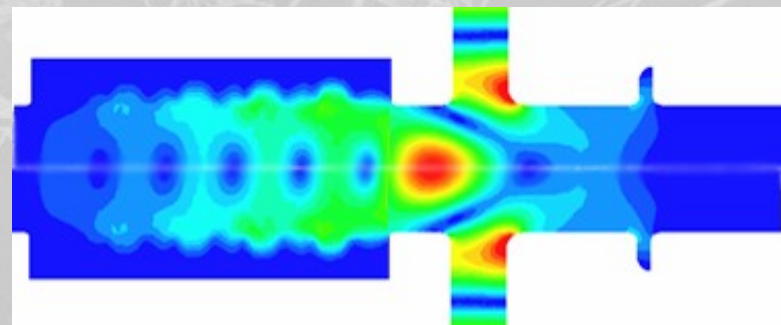
- not many 135+ MW X-band power sources – ASTA at SLAC
- much harder to run, full fields at input

Beam-based tests with CTF3 4-30 A beam.

- 1000 mm long PETS
- Connect output to input – beam-driven rf resonant ring for lower, <10 A, current



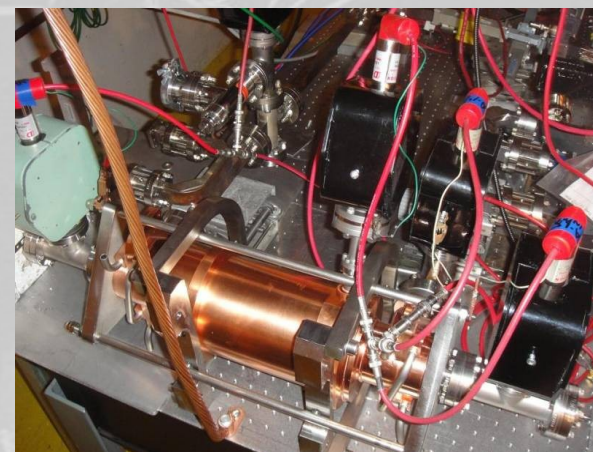
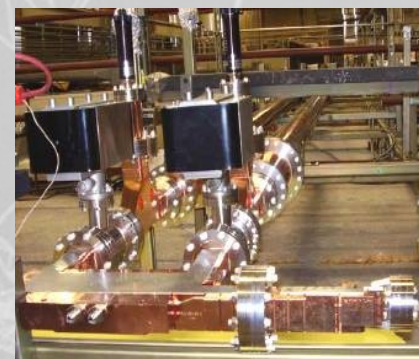
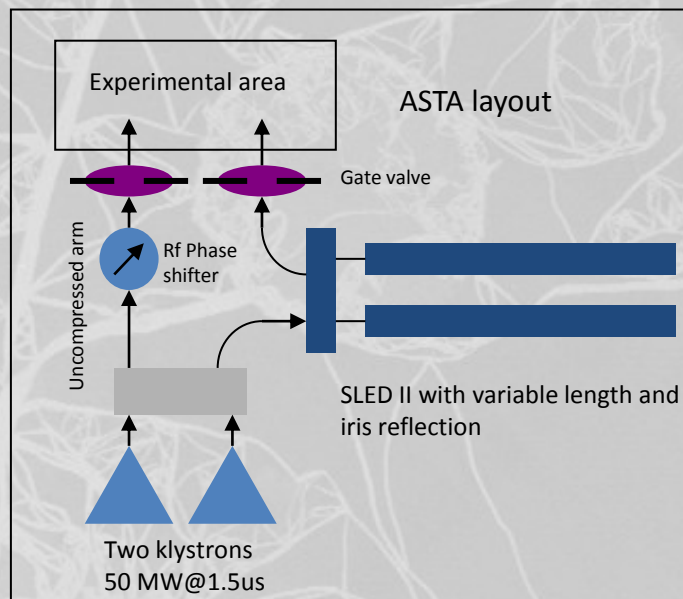
Fields in klystron and recirculation tests



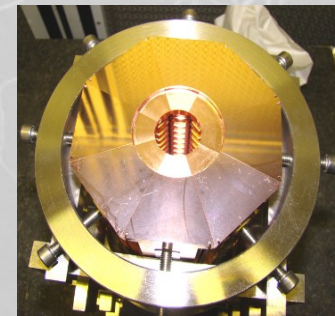
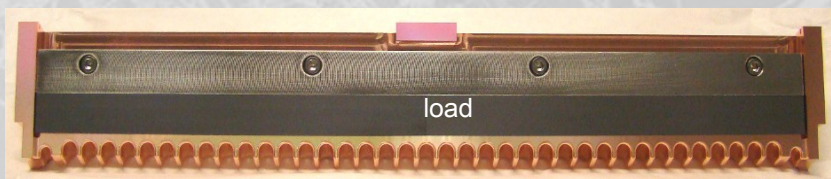
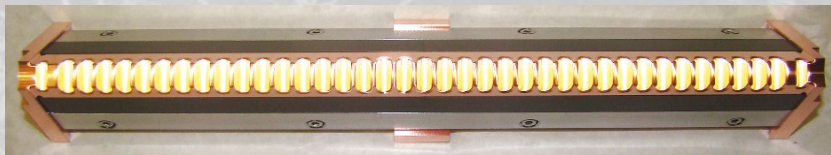
Fields in CLIC and CTF3 at high current

PETS testing in ASTA

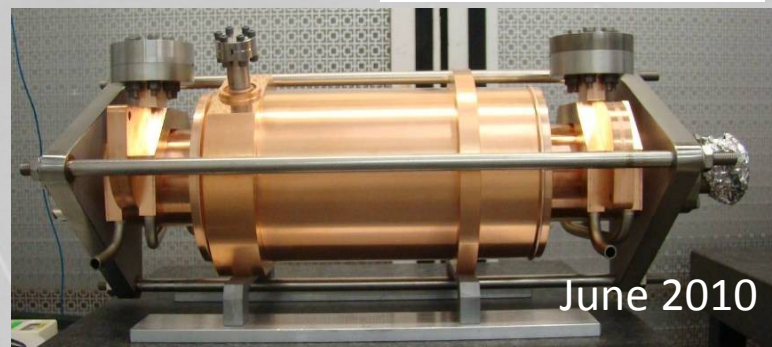
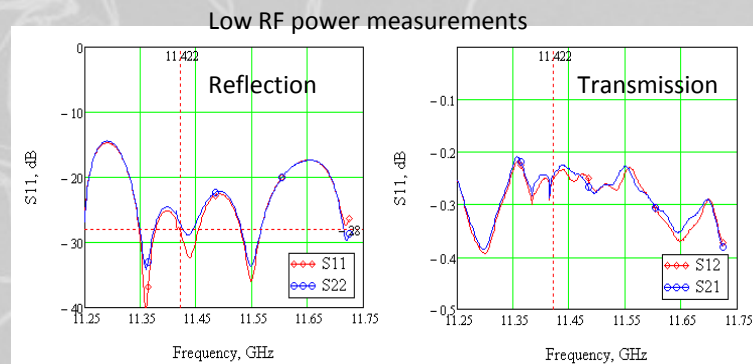
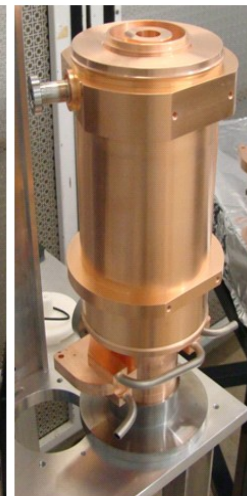
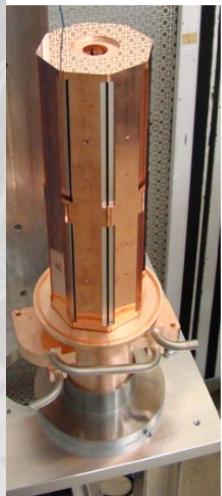
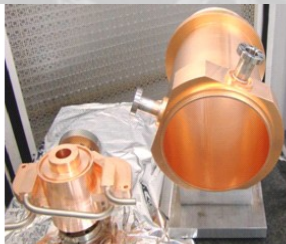
PETS waveguide-mode PETS testing is being done at ASTA in SLAC an impressive facility but testing a single object with 135+ MW power is very challenging. The results you will see are a mixture of conditioning of the PETS and ASTA...



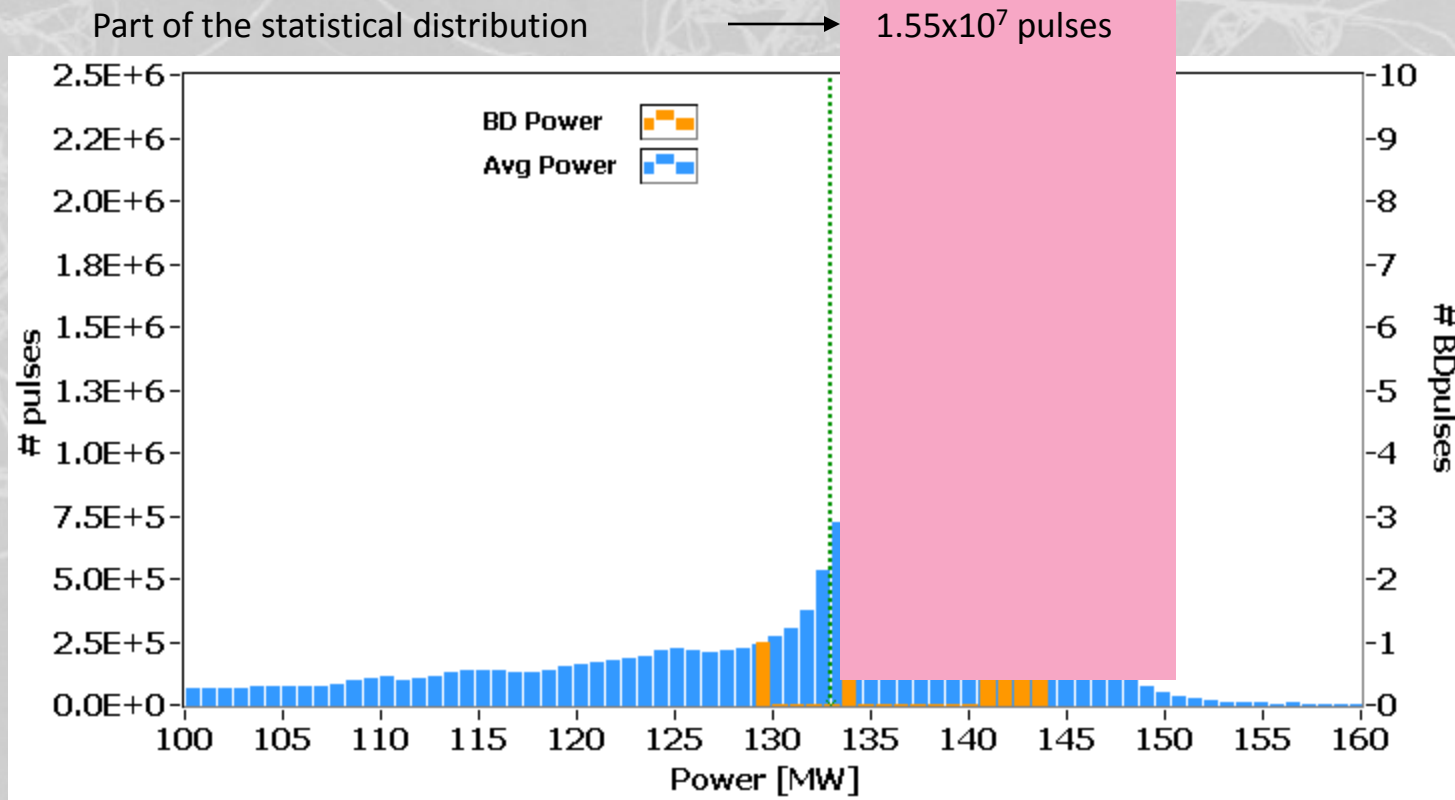
ASTA test PETS version with damping slots and damping material (SiC)



PETS preparation for the EB welding of the RF couplers and the mini-tank



June 2010



- 1.55x10⁷ pulses were accumulated in a 125 hour run.
- 8 PETS breakdowns were identified giving a breakdown rate of **5.3x10⁻⁷/pulse**.
- Most of the breakdowns were located in the upper tail of the distribution, which makes BDR estimate rather conservative.
- During the last 80 hours no breakdowns were registered giving a BDR **<1.2x10⁻⁷/pulse**.



Accelerating structures – specifications



High-gradient:

1. 100 MV/m loaded gradient
2. 170 (flat top)/240 (full) ns pulse length
3. $<4 \times 10^{-7}$ /pulse/m breakdown rate

Beam dynamics:

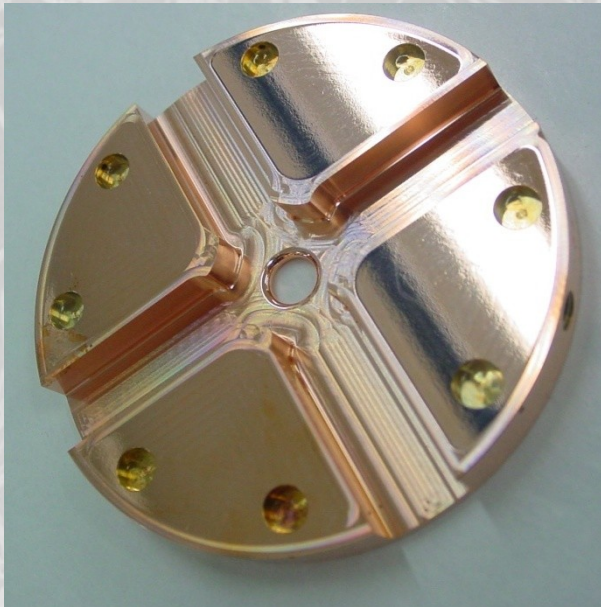
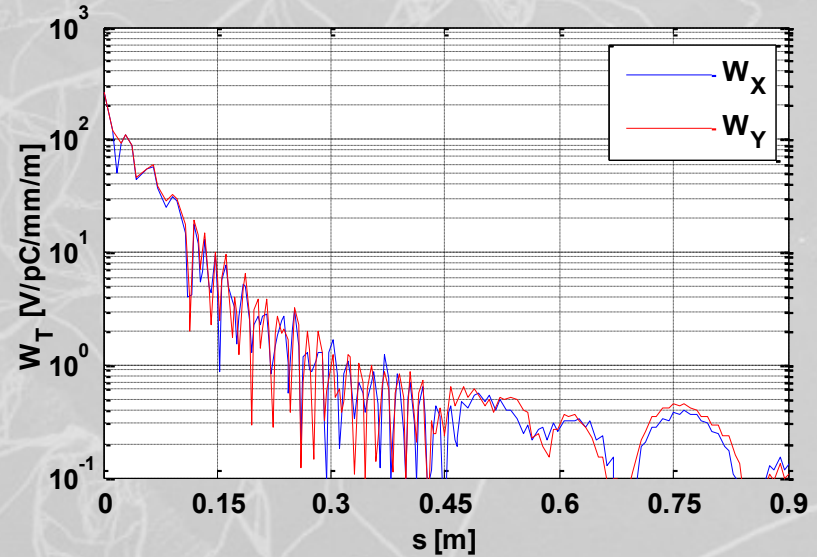
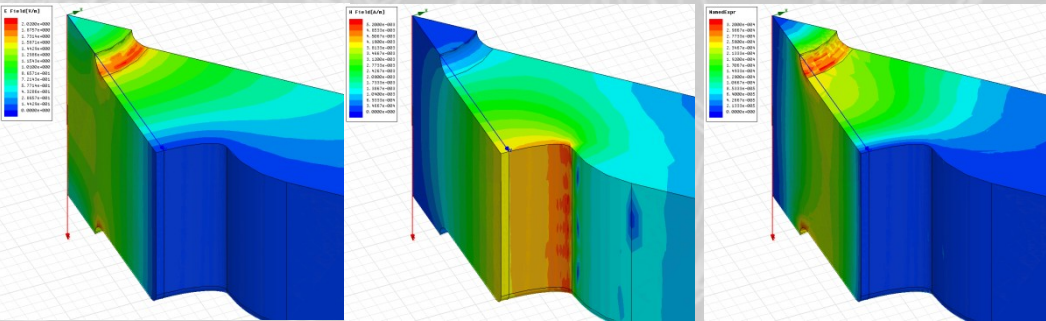
1. 5.8 mm diameter minimum average aperture (short range transverse wake)
2. < 1 V/pC/mm/m long-range transverse wakefield at second bunch (approximately x50 suppression).

Accelerating structures – features

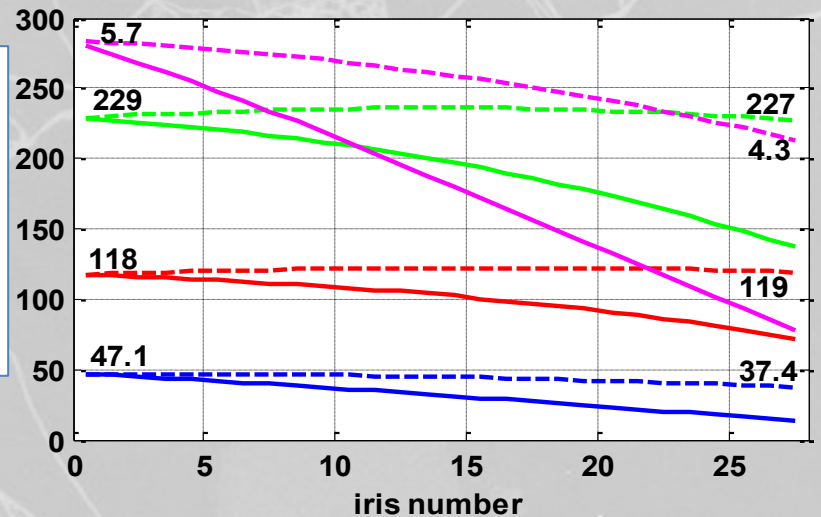
$$E_s/E_a$$

$$H_s/E_a$$

$$S_c/E_a^2$$



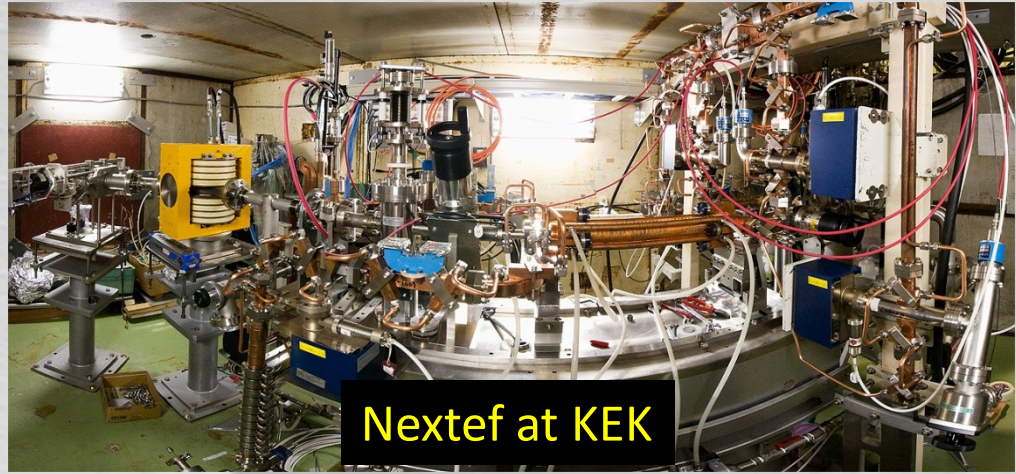
$S_c^{1/2}$ [MW/mm²]
 E_s max [MV/m]
 E_{acc} [MV/m]
 ΔT [°C]
 dashed – unloaded
 solid – loaded



Prototype accelerating structure test areas



NLCTA at SLAC



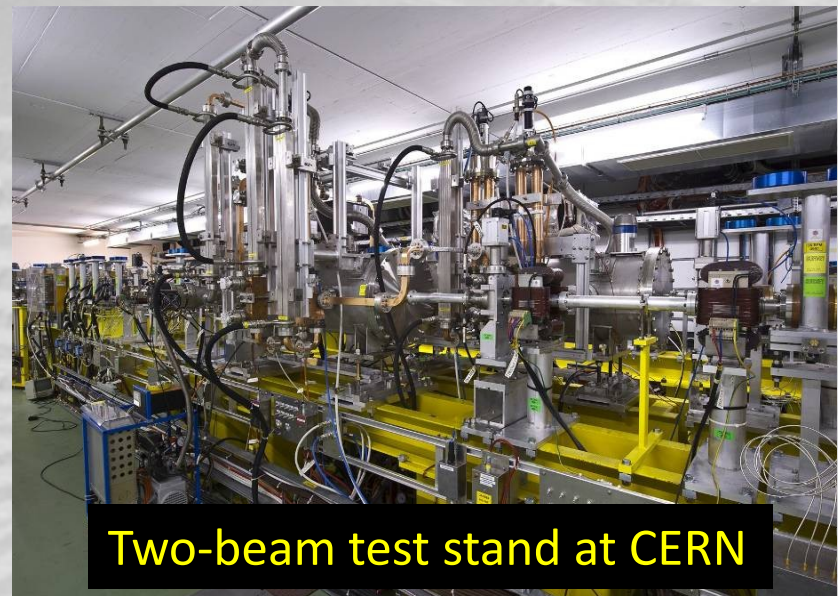
Nextef at KEK



New klystron at CERN



ASTA at SLAC



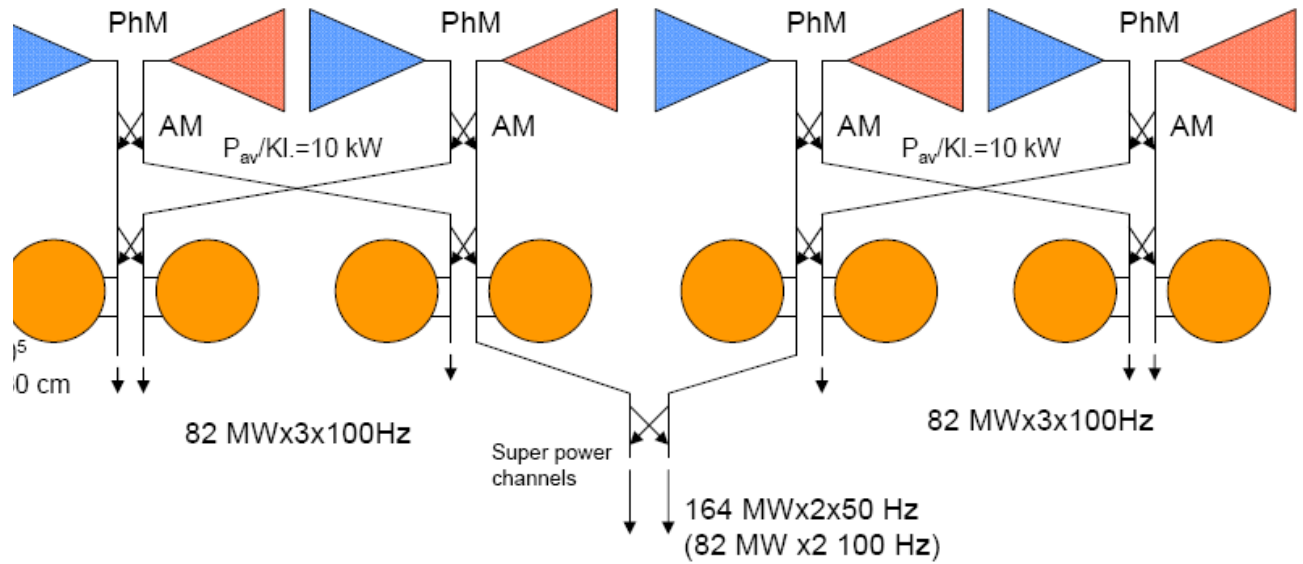
Two-beam test stand at CERN

A better way to expand testing capability?

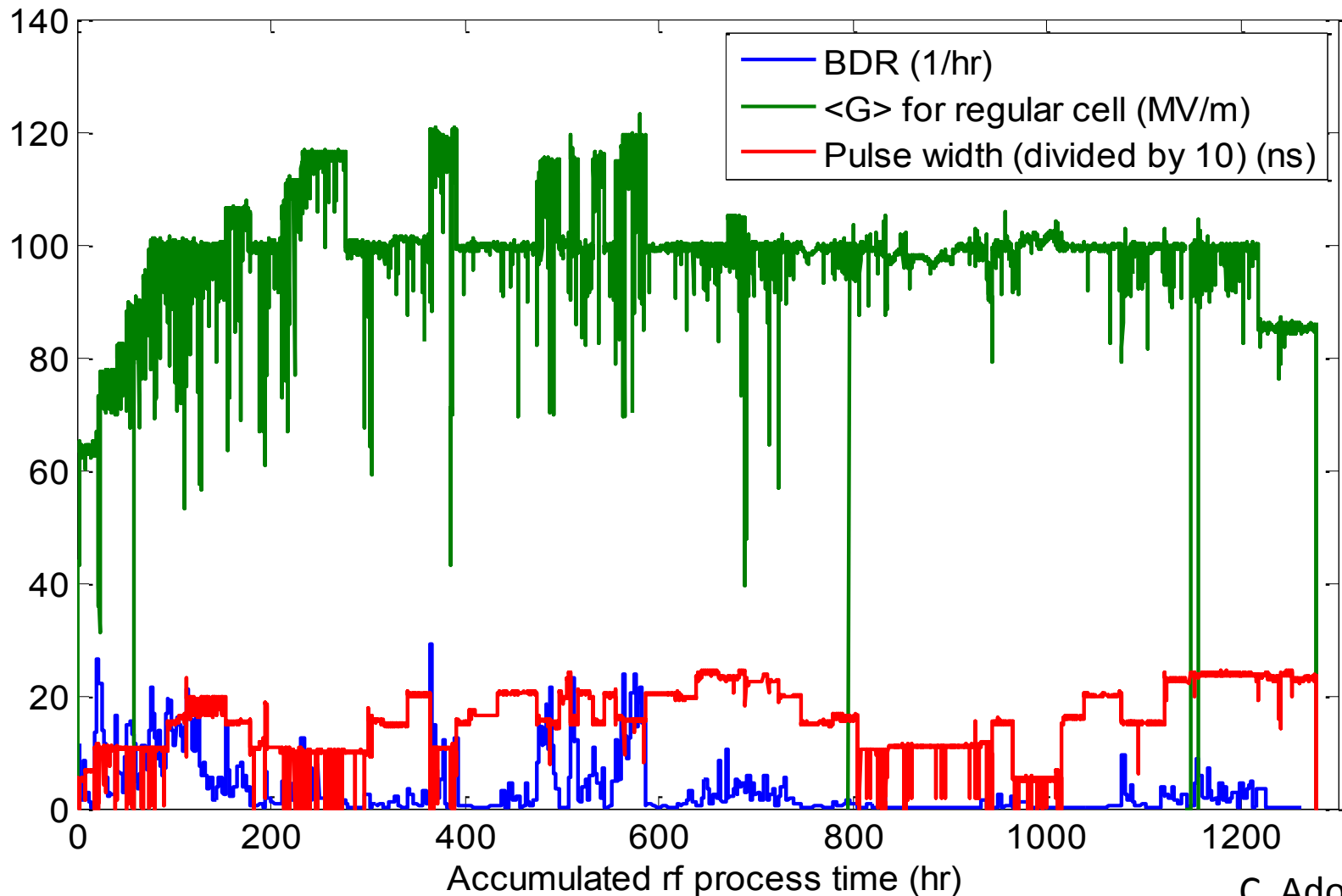


Layout of the multipurpose 12 GHz RF power station

12 GHz (5.5 MW x 4.6 μ sec x 400 Hz) x 8 klystrons (4 modulators)



High Power Operation History



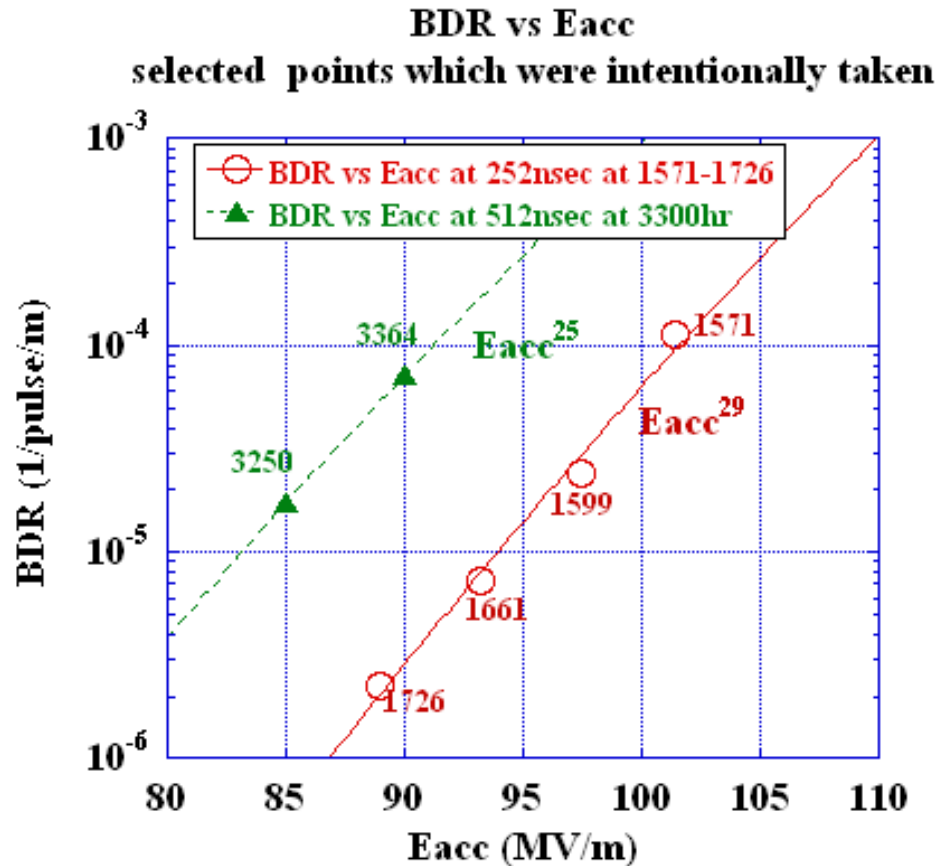
Final Run at 230 ns: 94 hrs at 100 MV/m w BDR = 7.6×10^{-5}
60 hrs at 85 MV/m w BDR = 2.4×10^{-6}

TD18

C. Adolphsen
F. Wang
SLAC

Relevant data points of BDR vs Eacc

101017



TD18

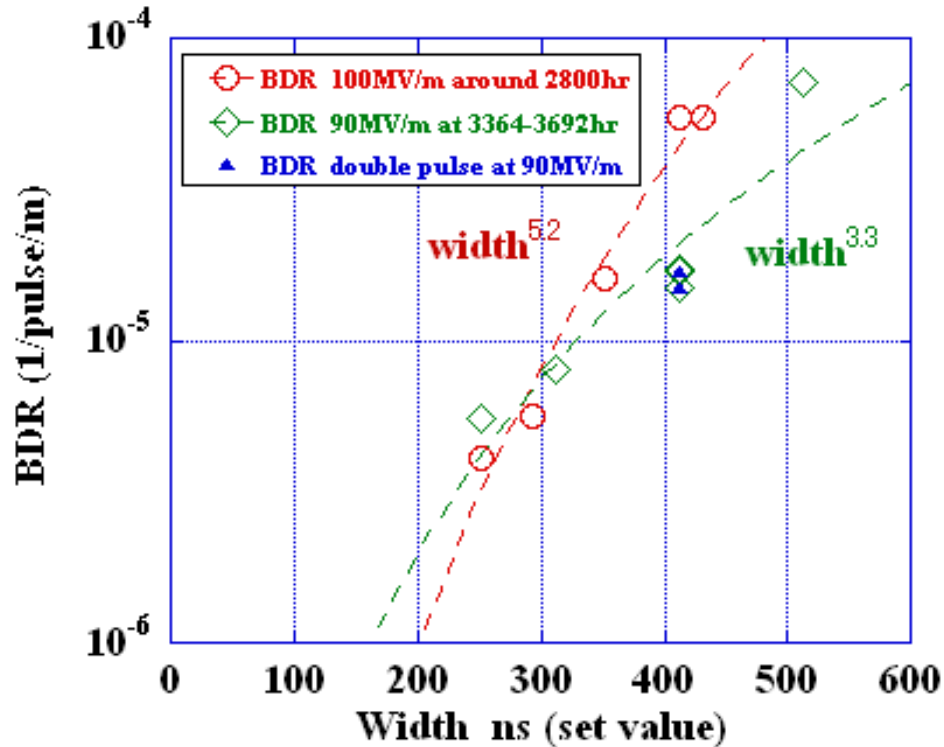
Step rise as Eacc, 10 times per 10 MV/m, less steep than T18

TD18_#2 BDR versus width

at 100MV/m around 2800hr and at 90MV/m around 3500hr

101017

TD18_Disk_#2 BDR vs Width



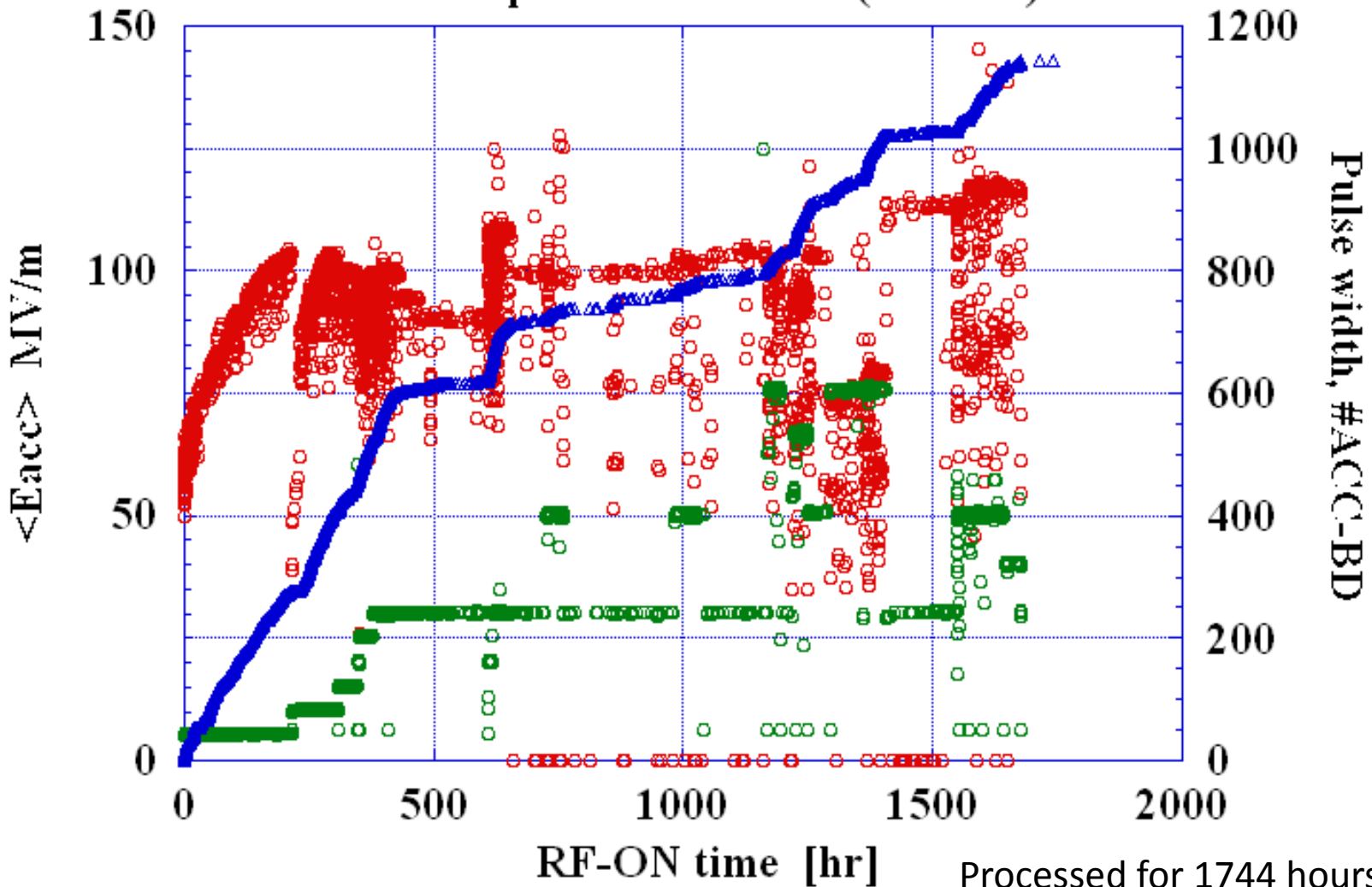
TD18

Similar dependence at 90 and 100 if take usual single pulse?

○ $\langle E_{acc} \rangle$ MV/m

T24#3 History run1-36 till earthquake on Mar. 11 (1744hrs)

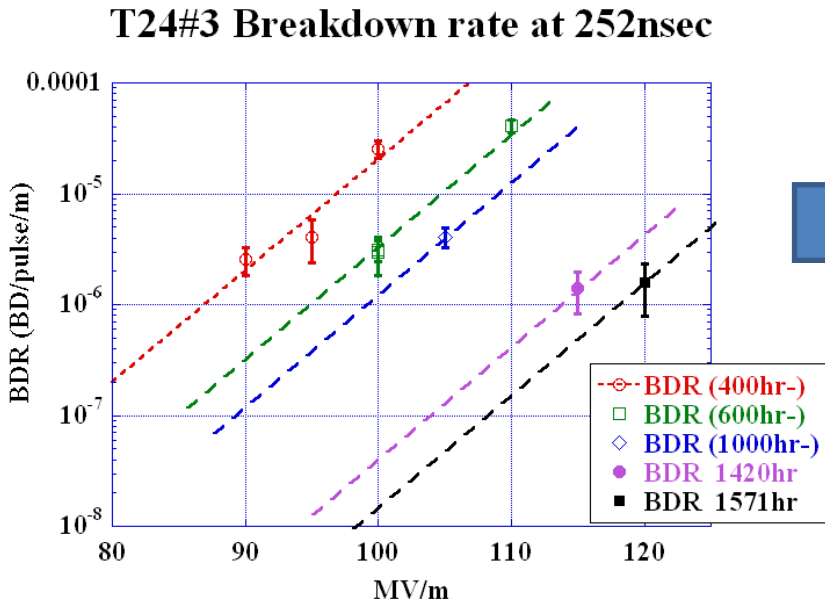
○ F50 width[ns]
△ #ACC-BD



Processed for 1744 hours.

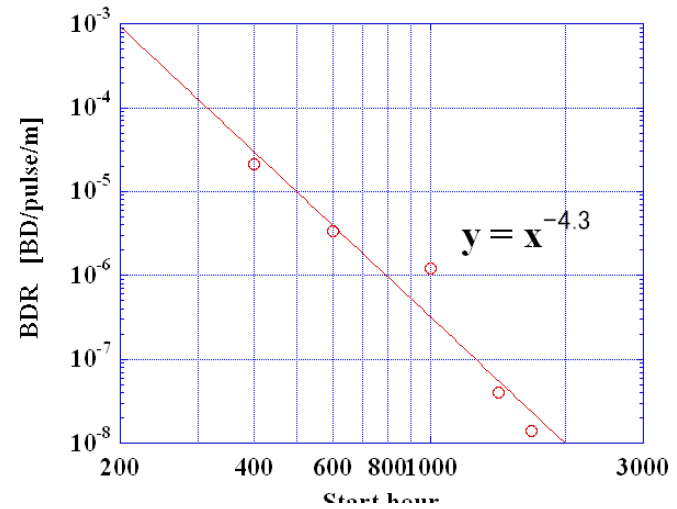
T24#3

BDR evolution at 252ns normalized 100MV/m

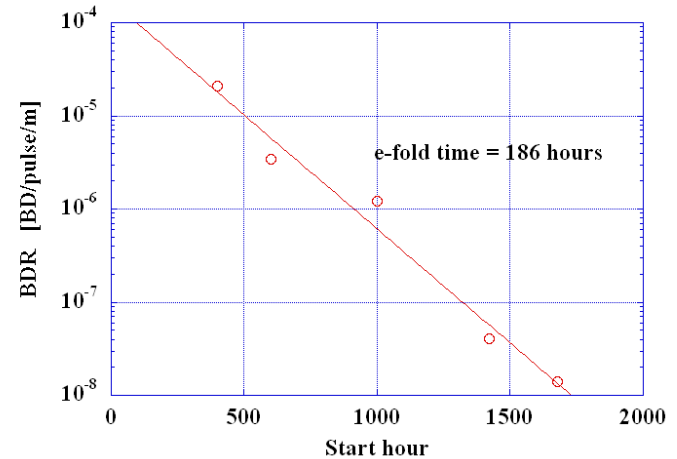


Assuming the same exponential slope as that at 400hr

T24#3 BDS vs time at 252ns 100MVm

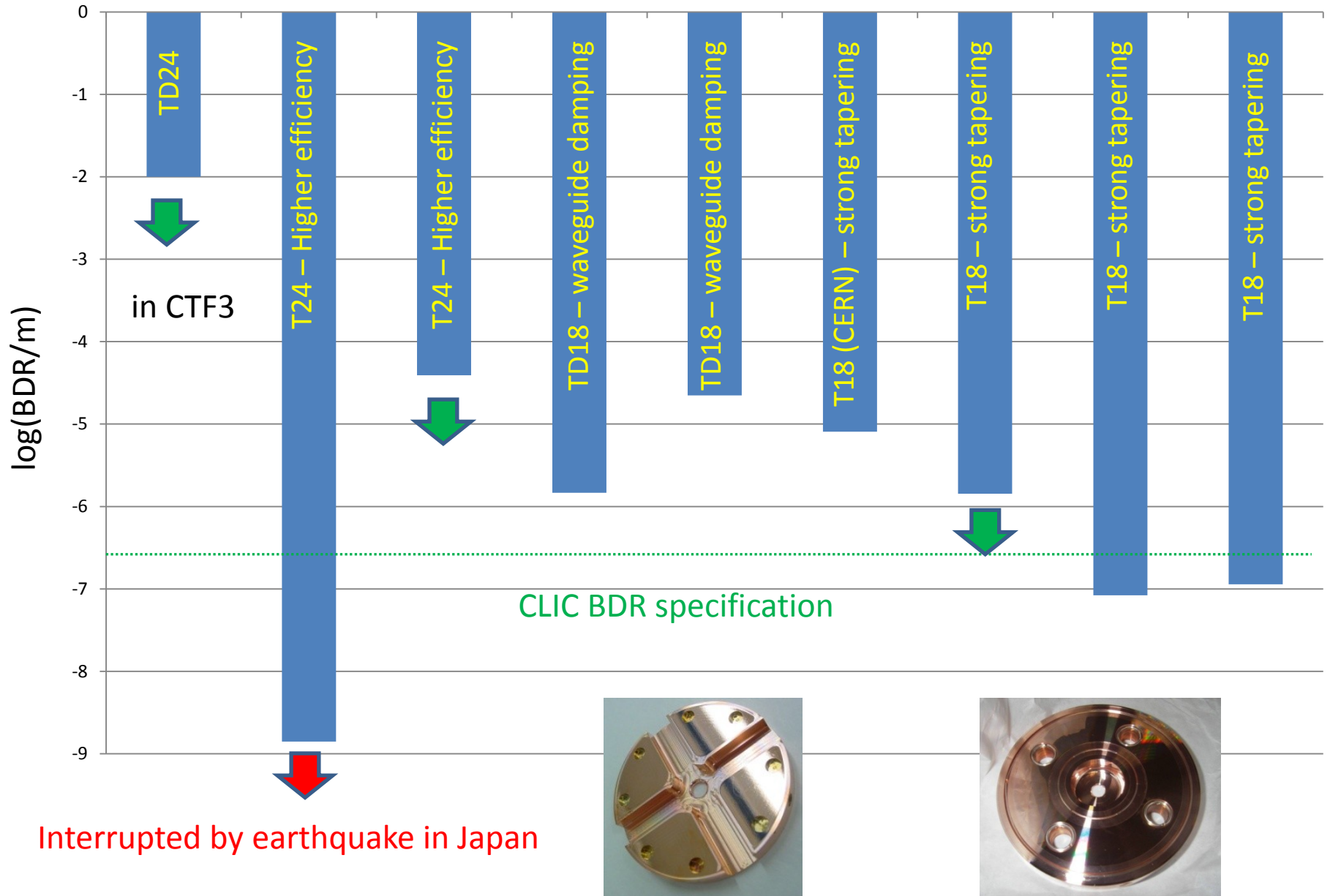


T24#3 BDS vs time normalized at 252ns 100MVm



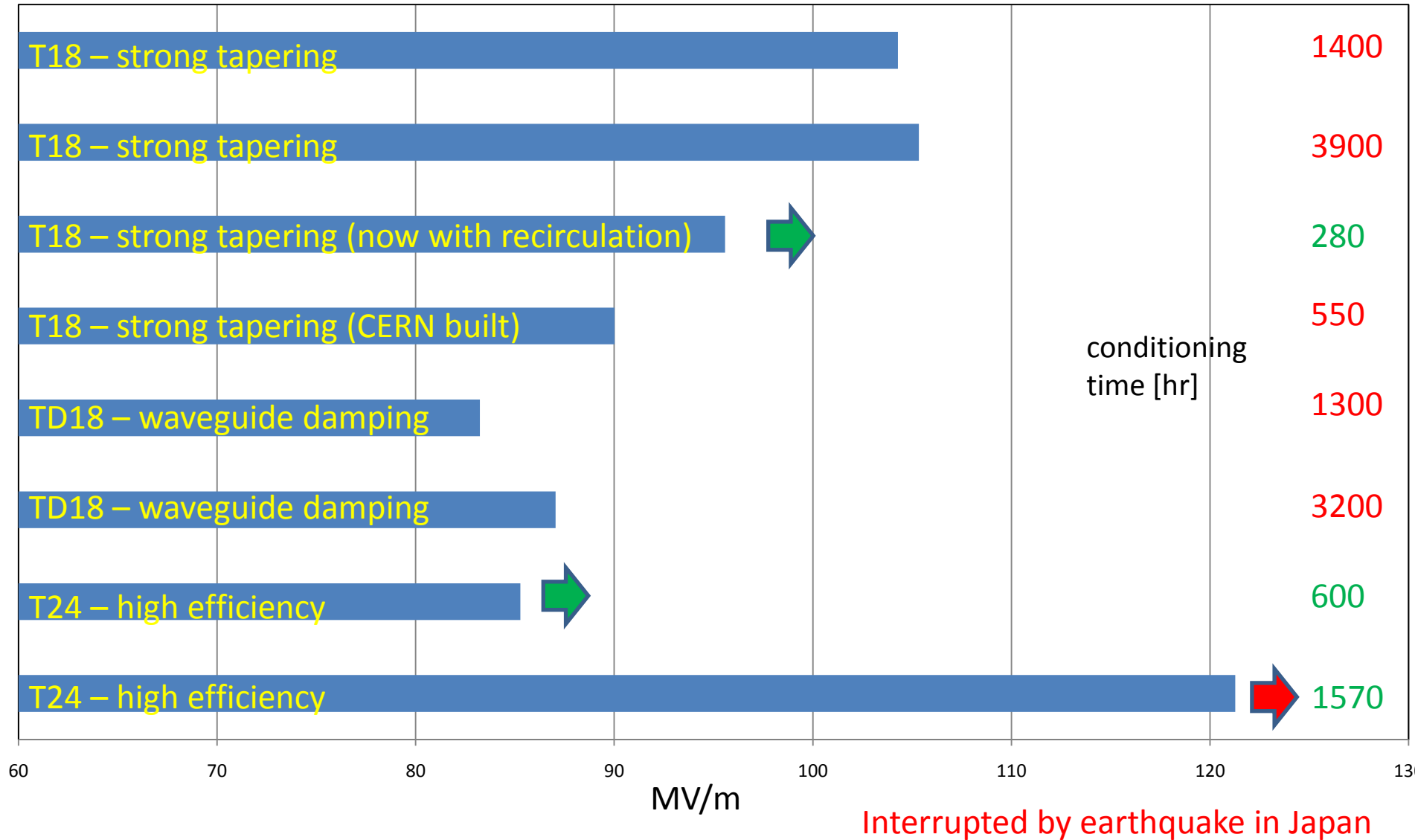
We understand the BDR has been kept decreasing.

Breakdown rate at 100 MV/m (unloaded) accelerating gradient and scaled to 180 ns pulse length



Interrupted by earthquake in Japan

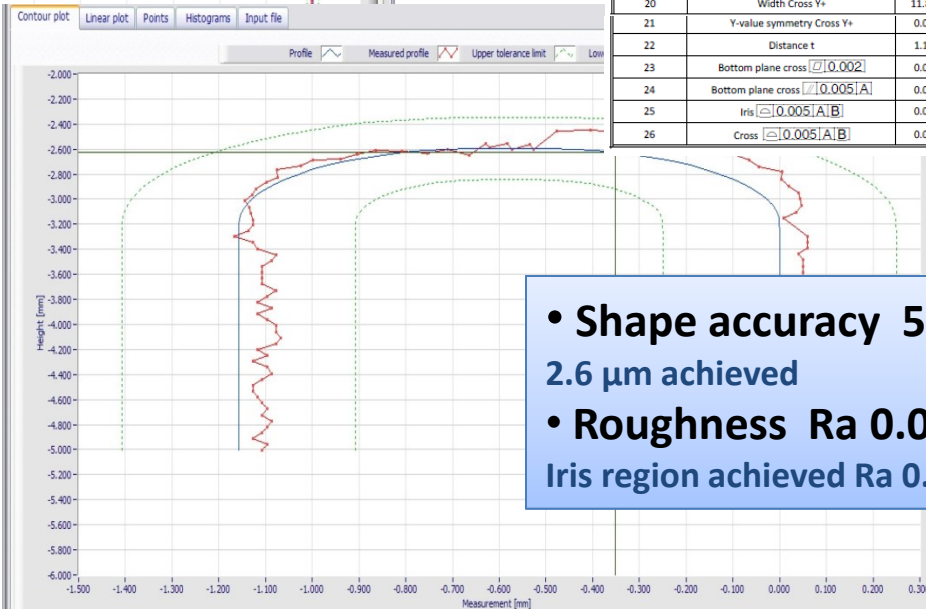
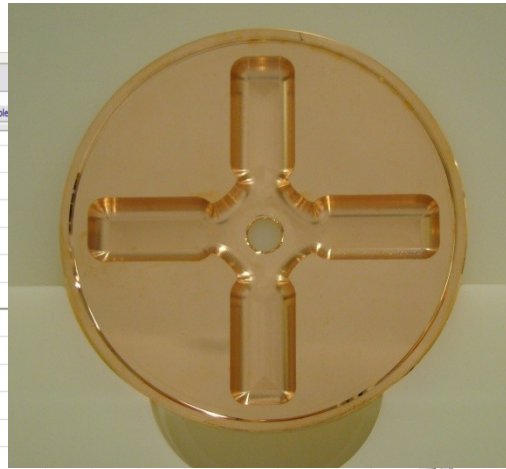
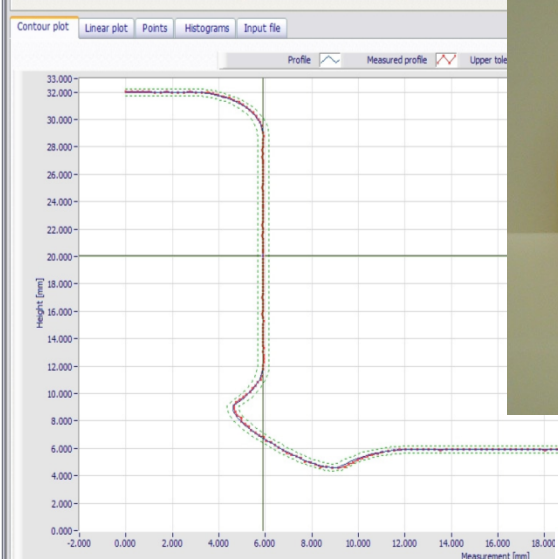
Unloaded gradient at CLIC $4 \cdot 10^{-7}$ BDR and 180 ns pulse length





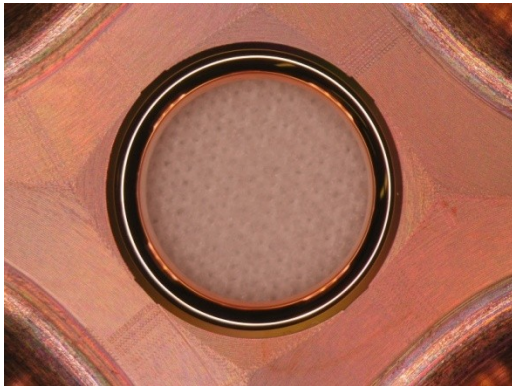
DETUNED DAMPED DISK FROM VDL (TD24)

germ



Enabling Technologies Group										Inspection Report	
Drawing no. CLIAAS110337 Standard Cell Disk Z1											Prod. Nr.
Description 11 WDSVDVGL8KEK Standard cell											
Dimensions											
Measurand	Description	Nominal	Upper	Lower	Actual	Deviation	Pass	Fail			
1	Ref A [Z]0.002	0.0000	0.0020	0.0000	0.0011	0.0011	✓	✗			
2	Outer diameter Ref B	74.0000	0.0025	-0.0025	74.0015	0.0015	✓	✗			
3	[Z]0.002	0.0000	0.0020	0.0000	0.0009	0.0009	✓	✗			
4	[Z]0.002[A]	0.0000	0.0020	0.0000	0.0006	0.0006	✓	✗			
5	ø 70	70.0000	0.0000	-0.0100	69.9957	-0.0043	✓	✗			
6	ø 70 [Z]0.005[B]	0.0000	0.0050	0.0000	0.0010	0.0010	✓	✗			
7	Diameter 2xa	5.1901	0.0025	-0.0025	5.1900	-0.0001	✓	✗			
8	Distance d	8.7327	0.0020	-0.0020	8.7334	0.0007	✓	✗			
9	Plane at distance d [Z]0.002	0.0000	0.0020	0.0000	0.0020	0.0020	✓	✗			
10	ø 70	70.0000	0.0150	0.0100	70.0133	0.0133	✓	✗			
11	ø 70 [Z]0.005[B]	0.0000	0.0050	0.0000	0.0007	0.0007	✓	✗			
12	Distance t	1.1569	0.0025	-0.0025	1.1562	-0.0007	✓	✗			
13	Distance g	7.5758	0.0025	-0.0025	7.5765	0.0007	✓	✗			
14	Width Cross Z+	11.8113	0.0025	-0.0025	11.8131	0.0019	✓	✗			
15	Y-value symmetry Cross Z+	0.0000	0.0025	-0.0025	0.0002	0.0002	✓	✗			
16	Width Cross Z-	11.8113	0.0025	-0.0025	11.8134	0.0022	✓	✗			
17	Y-value symmetry Cross Z-	0.0000	0.0025	-0.0025	0.0002	0.0002	✓	✗			
18	Width Cross Y-	11.8113	0.0025	-0.0025	11.8122	0.0009	✓	✗			
19	Y-value symmetry Cross Y-	0.0000	0.0025	-0.0025	0.0012	0.0011	✓	✗			
20	Width Cross Y+	11.8113	0.0025	-0.0025	11.8120	0.0007	✓	✗			
21	Y-value symmetry Cross Y+	0.0000	0.0025	-0.0025	0.0003	0.0003	✓	✗			
22	Distance t	1.1569	0.0025	-0.0025	1.1563	-0.0006	✓	✗			
23	Bottom plane cross [Z]0.002	0.0000	0.0050	0.0000	0.0005	0.0005	✓	✗			
24	Bottom plane cross [Z]0.005[A]	0.0000	0.0025	-0.0025	0.0014	0.0014	✓	✗			
25	Iris [Z]0.005[A][B]	0.0000	0.0050	0.0000	0.0026	0.0026	✓	✗			
26	Cross [Z]0.005[A][B]	0.0000	0.0050	0.0000	0.0027	0.0027	✓	✗			

Zeiss CMM, free state measurement

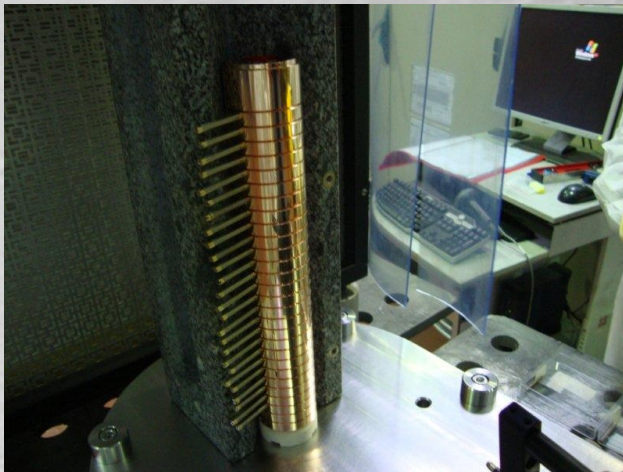


- Shape accuracy 5 µm
- 2.6 µm achieved
- Roughness Ra 0.025
- Iris region achieved Ra 0.016

Individual inspection



Operation done under laminar flow



Boxes under N2

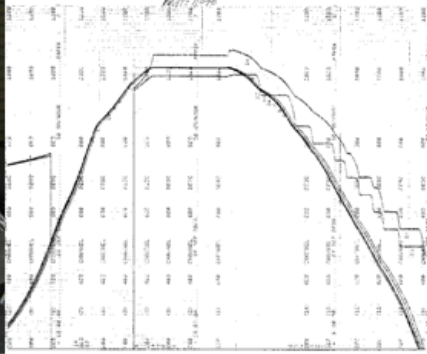
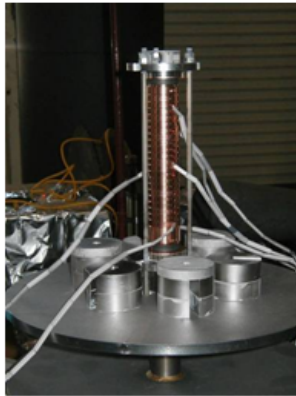


Sealed bag under N2

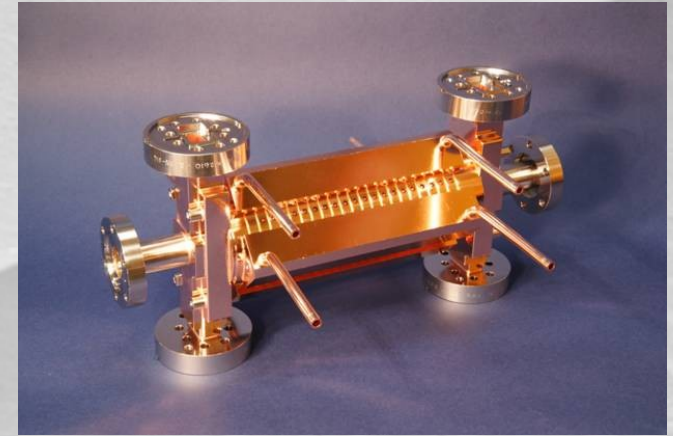
RF measurement



Diffusion Bonding of T18_vg2.4_DISC



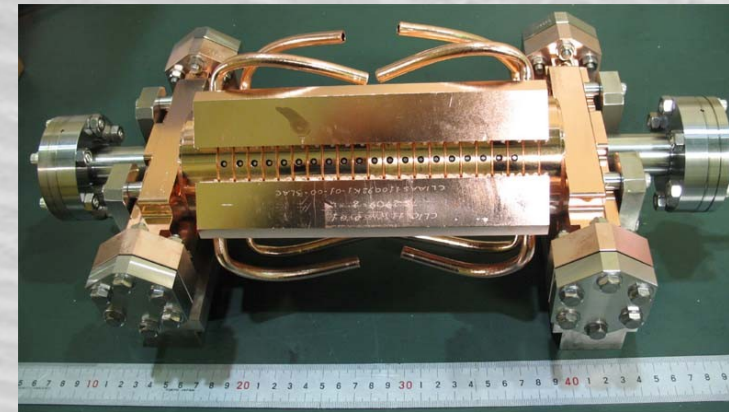
Pressure: 60 PSI (60 LB for this structure disks)
Holding for 1 hour at 1020°C



Vacuum Baking of T18_vg2.4_DISC



650°C
10 days



Stacking disks

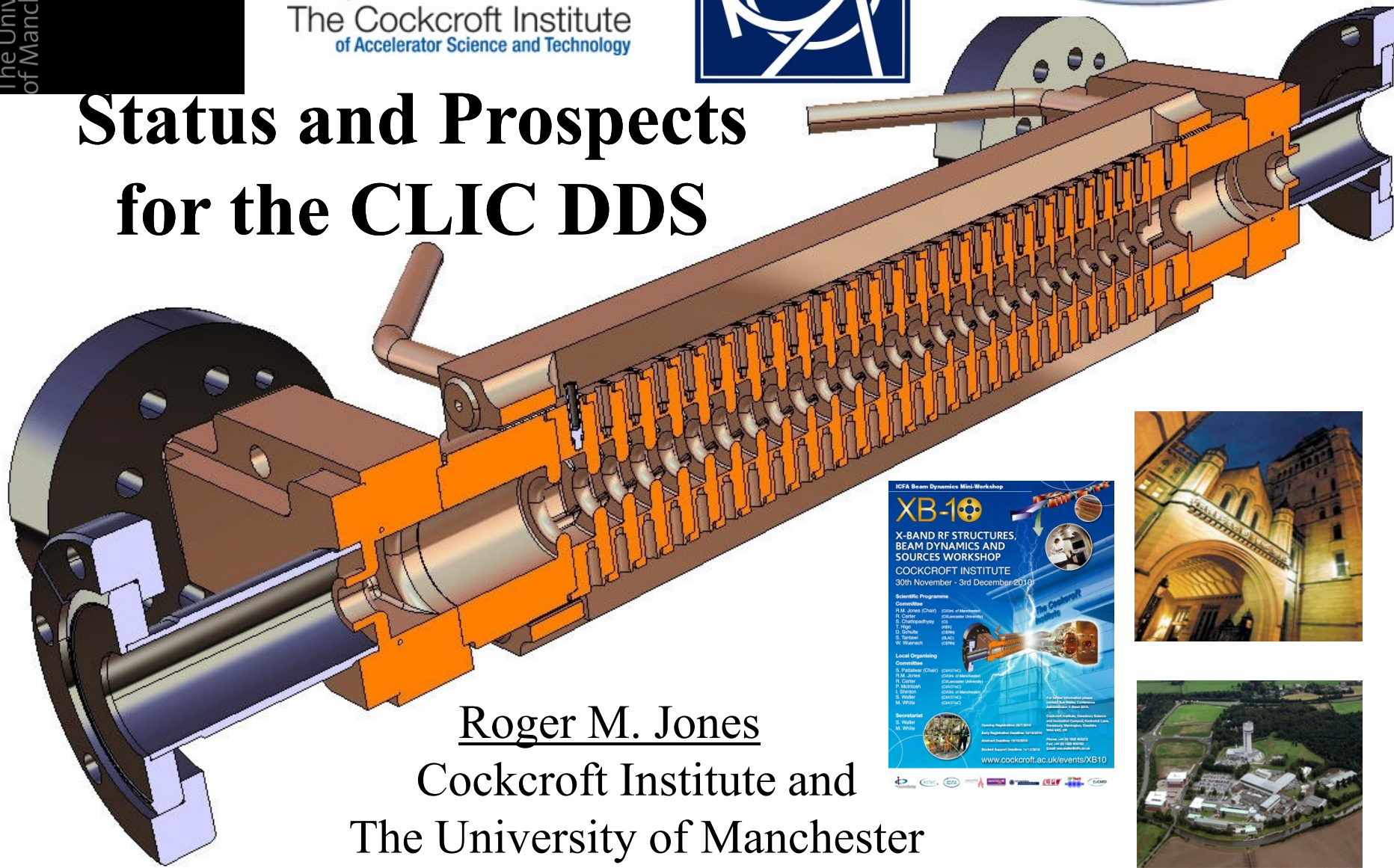
Structures ready for test

Temperature treatment for high-gradient

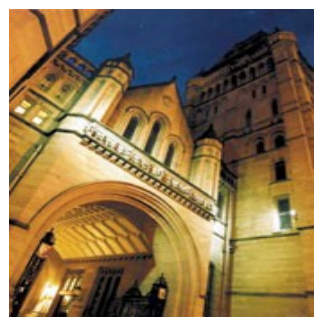
Walter Wuensch

30 November 2010

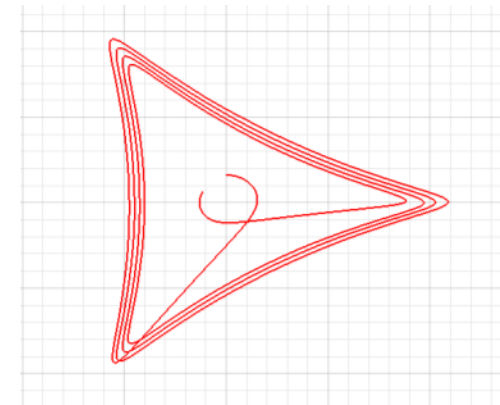
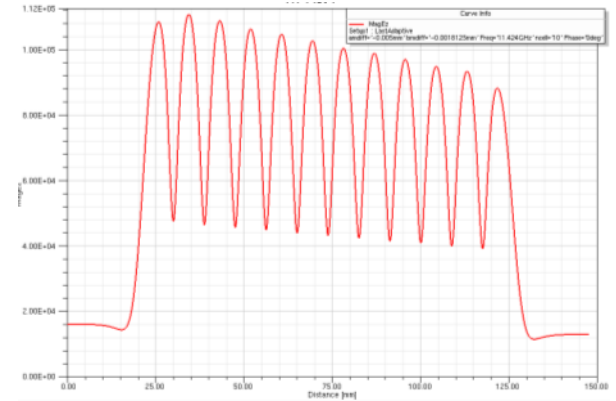
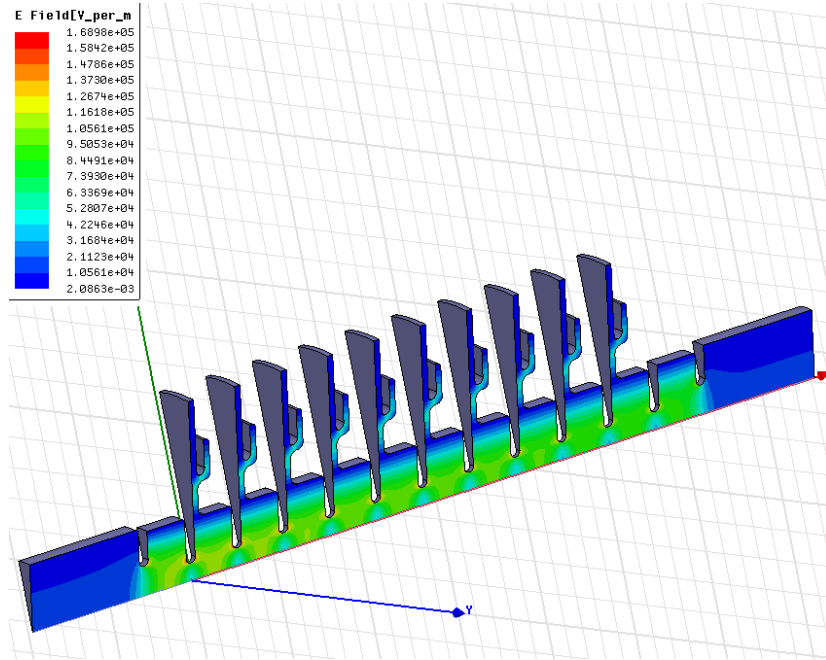
Status and Prospects for the CLIC DDS



Roger M. Jones
Cockcroft Institute and
The University of Manchester



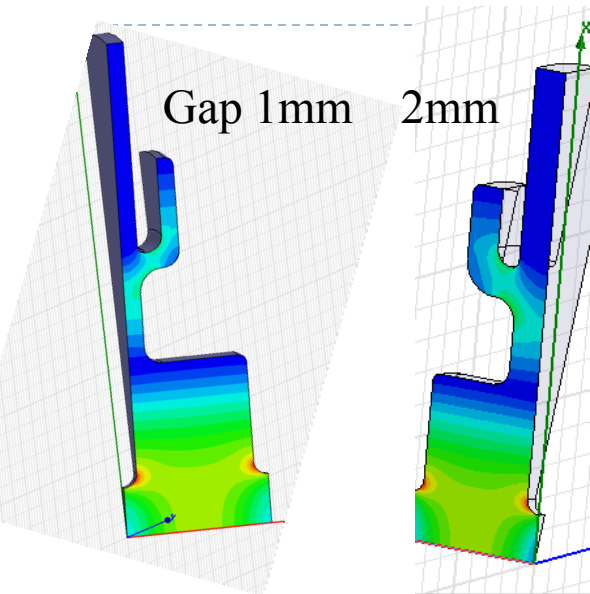
Design of CD-10-Choke



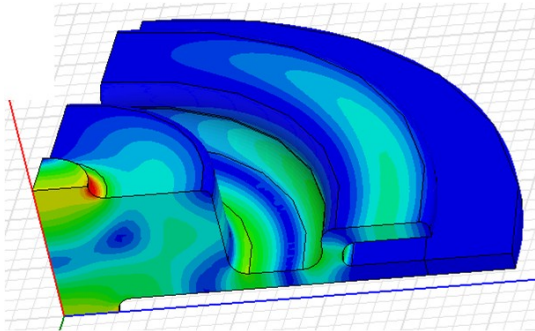
120 Degree

- ▶ CD10-Choke for demonstration
 - ▶ RF Design for Gap 1mm, 1.5mm, 2mm
 - ▶ Mechanical Design finished for 1mm-gap
 - ▶ Qualification disks and bonding test
- ▶ To the production pipeline and High Power testing

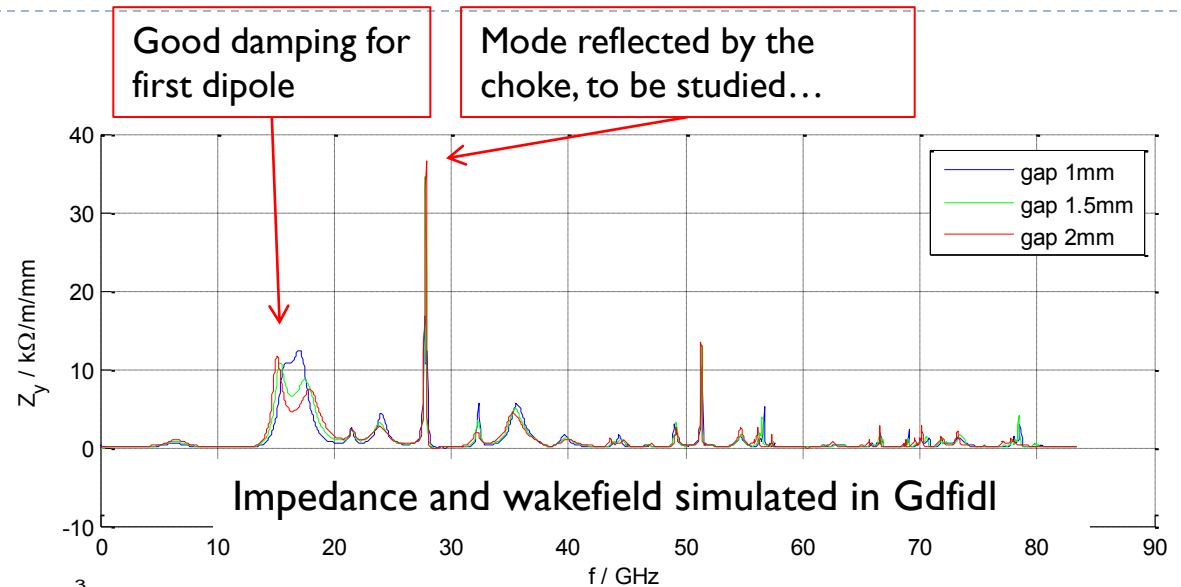
Damping simulation with Gdfid1/HFSS



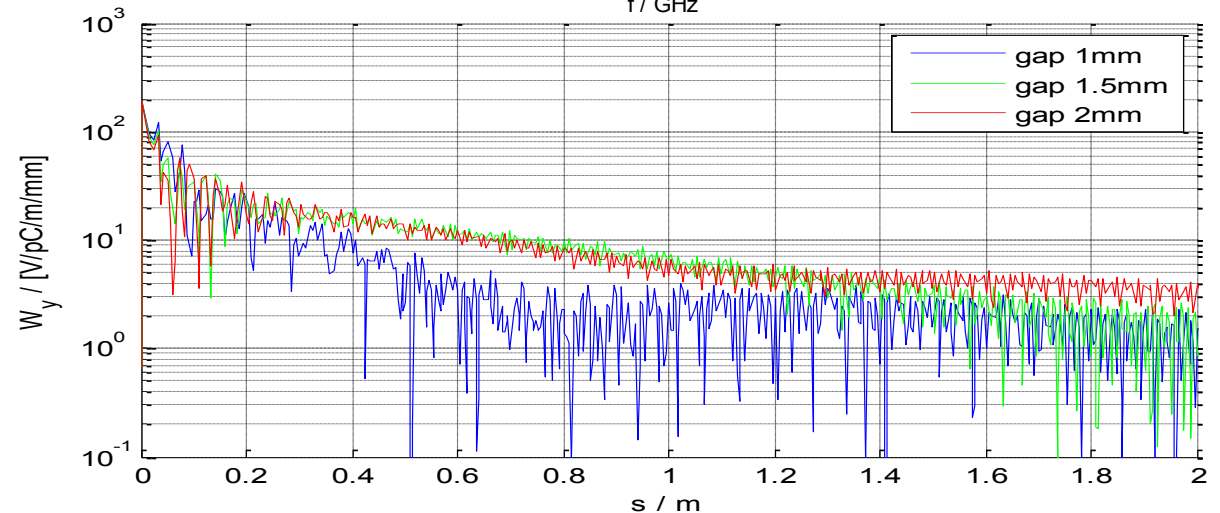
E field, fundamental mode



E field of a dipole mode that is reflected by the choke



Impedance and wakefield simulated in Gdfid1



CLIC main linac rf network

PETS

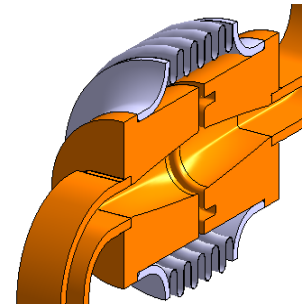
- high-power
- as short as possible
- low longitudinal and transverse impedance

Waveguide network

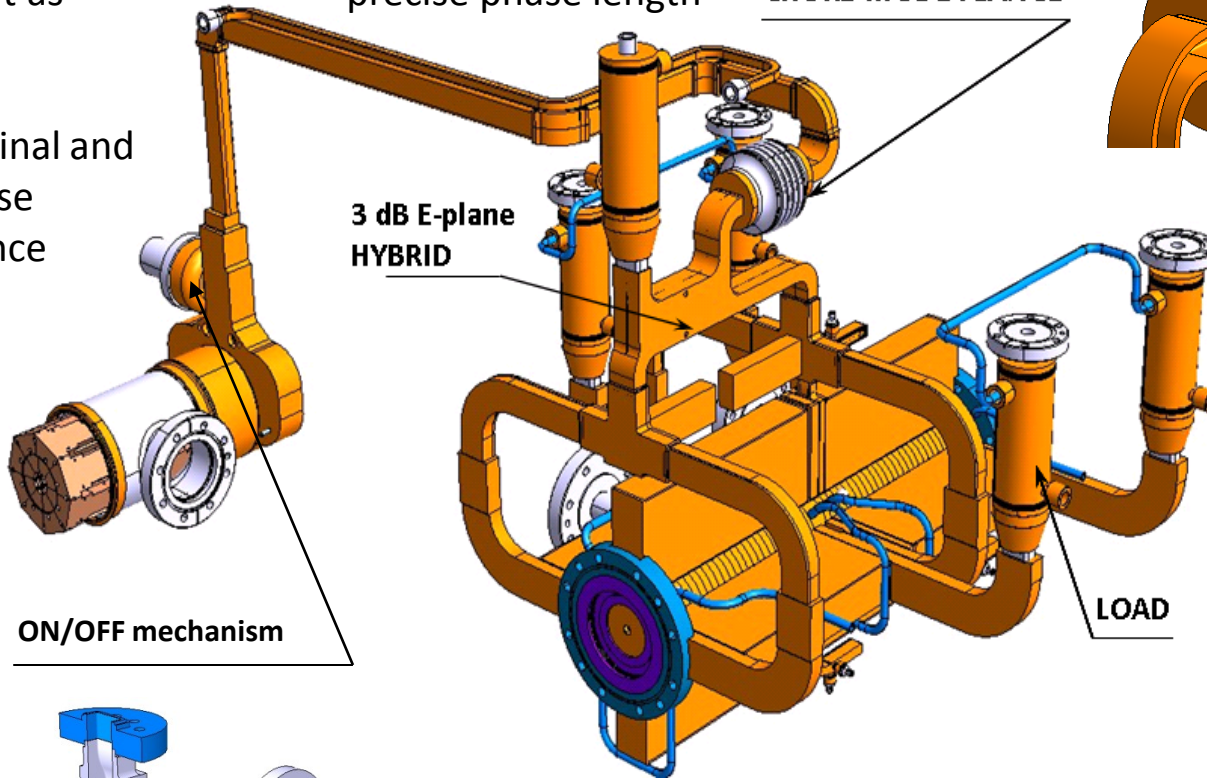
- high power
- precise phase length

CHOKE-MODE FLANGE

3 dB E-plane HYBRID

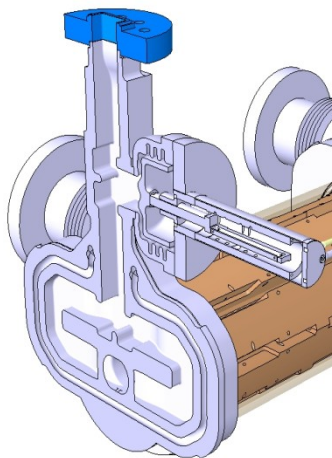


Choke mode flange
• independent alignment of main and drive beam



ON/OFF mechanism

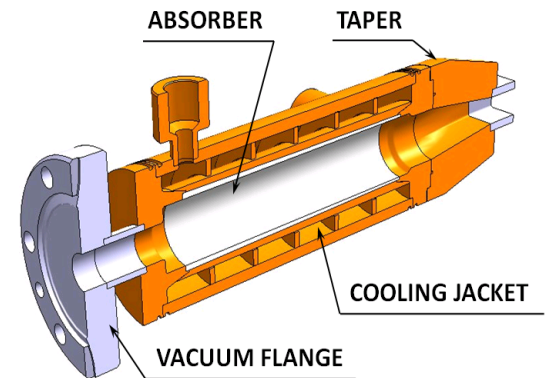
LOAD



On/ramp/off
• necessary (?) to react to breakdown and/or failure

Accelerating structure

- high-gradient
- as long as possible
- micron precision
- transverse wakefield suppression



ABSORBER

TAPER

COOLING JACKET

VACUUM FLANGE



High-power design criteria



We have developed a set of high-power scaling laws to describe the observed dependence which are supported by plausible physical arguments:

$$\frac{P}{C} \propto \text{const}$$

global power flow

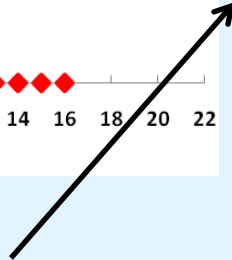
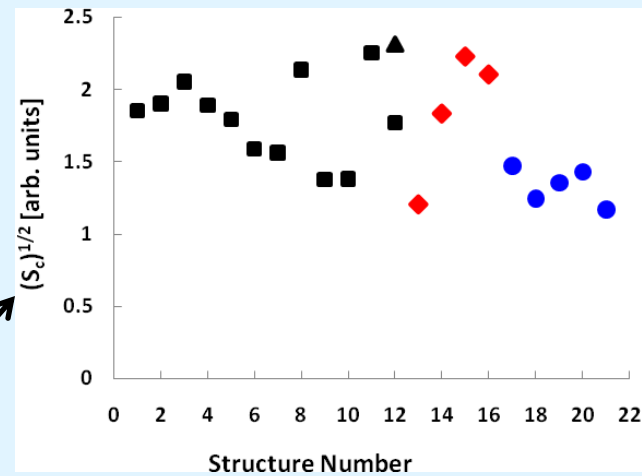
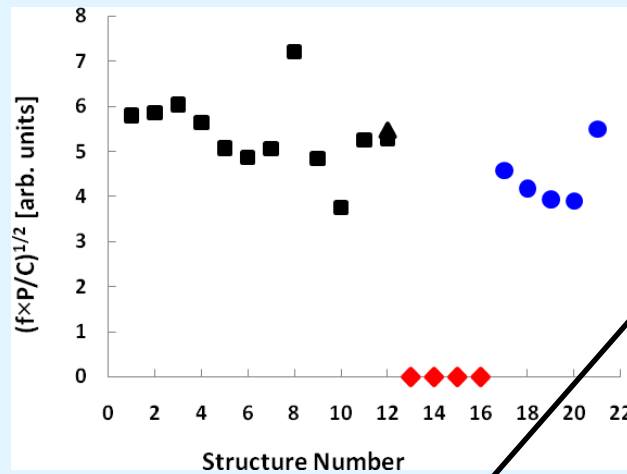
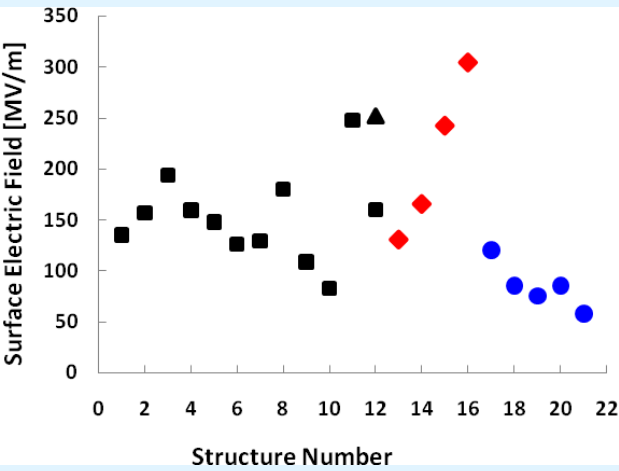
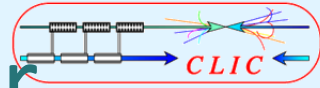
$$S_c = \text{Re}(\mathbf{S}) + 6 \text{Im}(\mathbf{S})$$

local complex power flow

These are now standard design criteria used throughout the CLIC structure program. We are actively pursuing checking their validity over a wider range of parameters and putting them on a more solid footing – fundamental breakdown studies later in this talk.



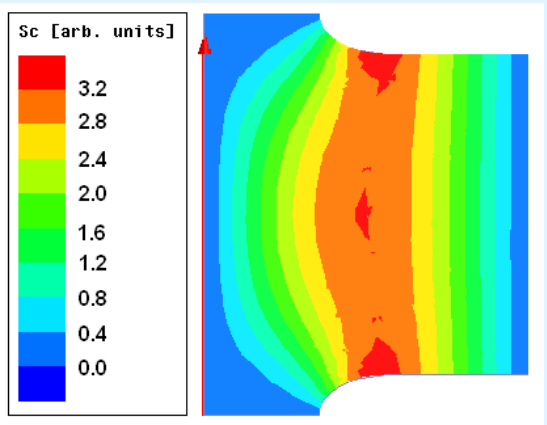
S_c : high-power design parameter



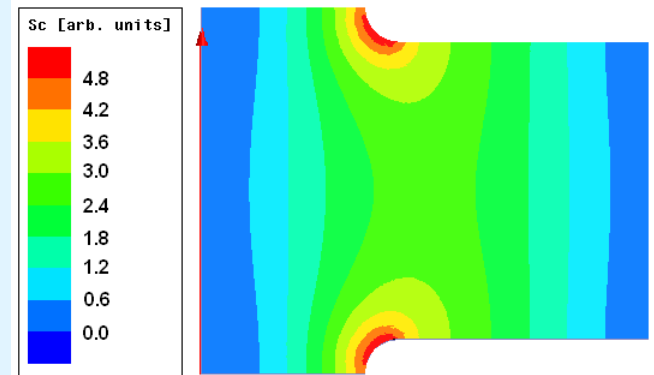
X-band and 30 GHz,
pulses of the order of
100 ns.
Travelling and standing
wave

Related to the complex Poynting vector:

$$S_c = \Re \{ \bar{S} \} + g_c \cdot \Im \{ \bar{S} \}$$



Travelling wave



Standing wave

W. Wuensch



Cavity Performance and RF Results

Silvia Verdú Andrés

U. Amaldi, R. Bonomi, A. Degiovanni,
M. Garlasché, R. Wegner

TERA Foundation

Do our high-gradient limits extend all the way down to S-band and microsecond pulses?
PRELIMINARY RESULTS!

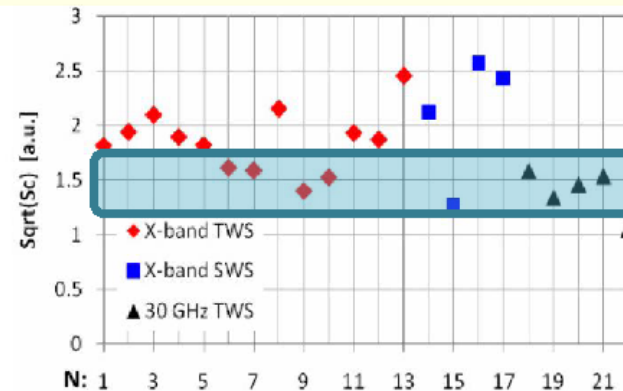
Validation of CLIC observations:

The modified Poynting vector as a RF constraint to high gradient performance

The square root of S_C has been scaled to $t_{pulse} = 200$ ns and $BDR = 10^{-6}$ bbp/m

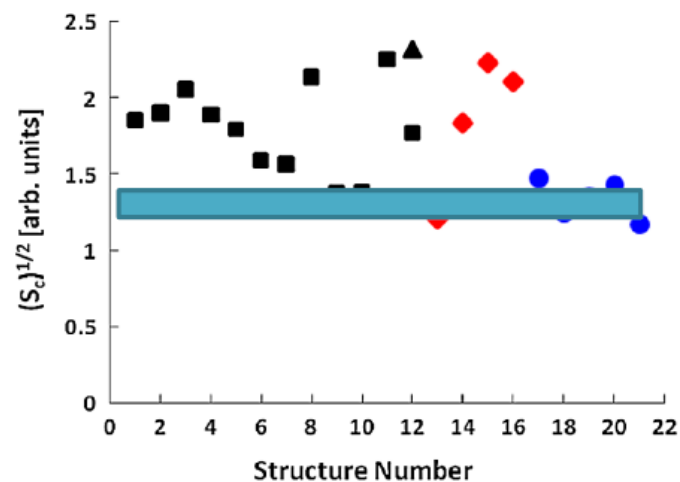
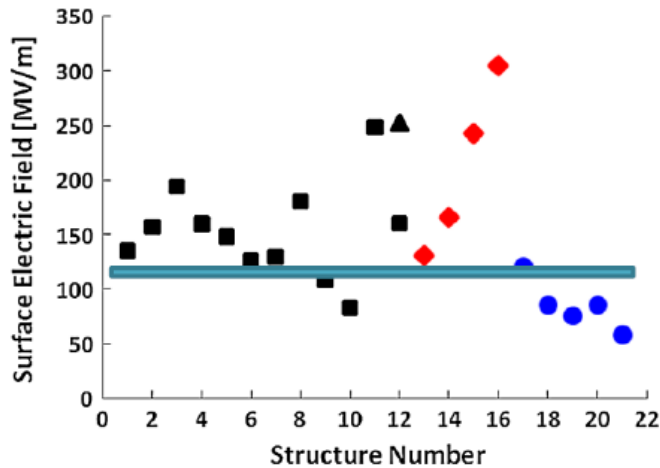
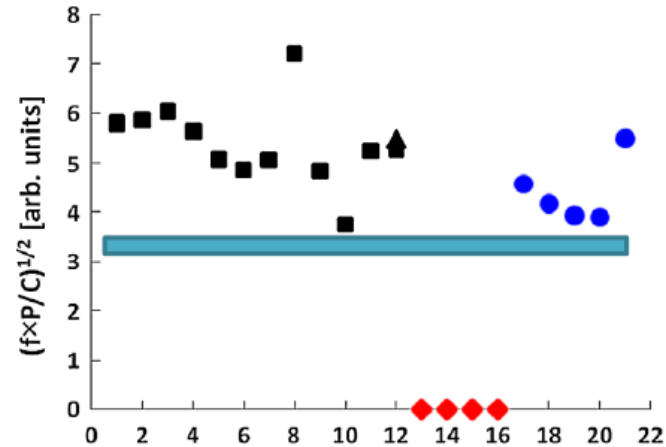
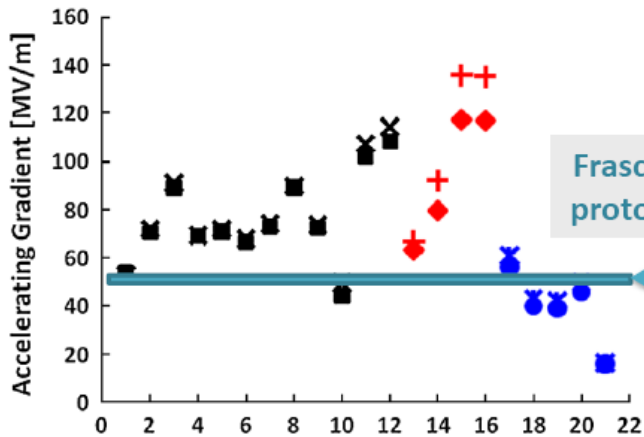
$$\sqrt{S_C^{scaled}} = \sqrt{S_C} \cdot \left(\frac{t_{pulse}}{t_{ref}} \right)^{\frac{1}{6}} \cdot \left(\frac{BDR^{ref}}{BDR} \right)^{\frac{1}{3}}$$

"A New Local Field Quantity Describing the High Gradient Limit of Accelerating Structures",
A.Grudiev et al., Phys.Rev.ST Accel. Beams (2009) 102001



← **TERA**
Sqrt(S_C) ∈ [1.3-1.6]

Results: *limit to high-gradient performance???*



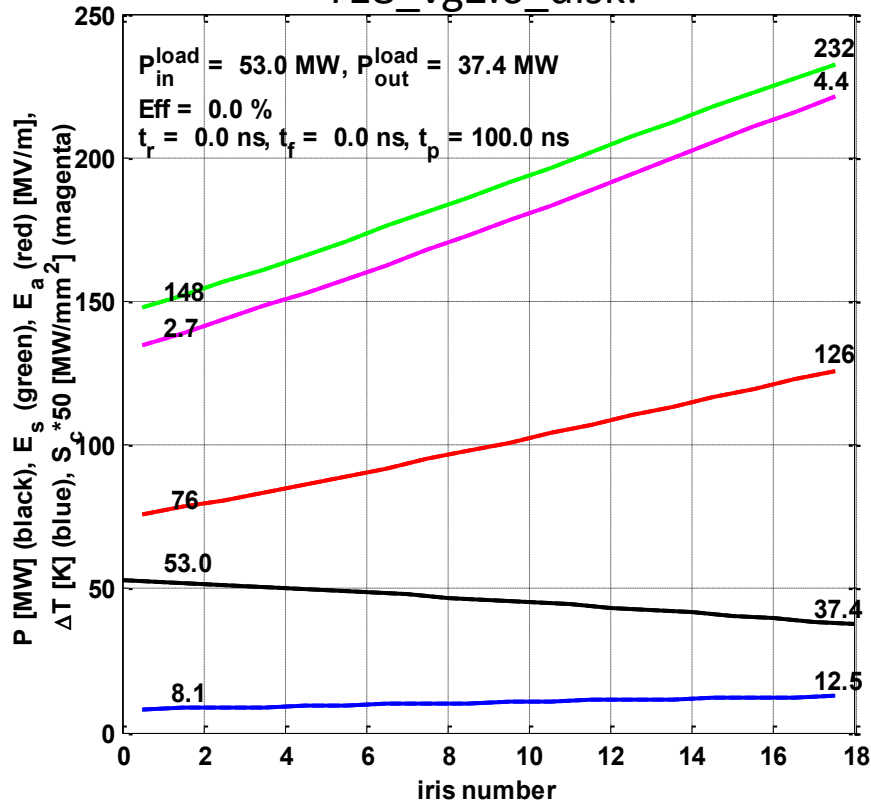
- great accordance with data for E_0 and E_s plots; lower accordance for P and S plots

1st generation of CLIC X-band test structure prototypes T18/TD18

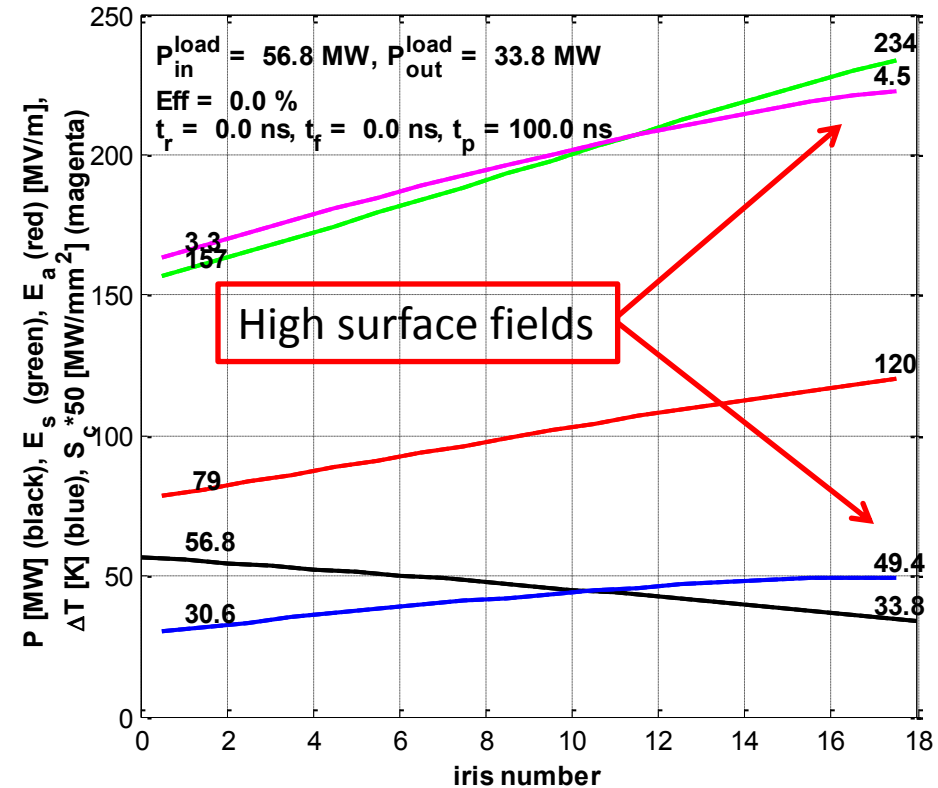
2007

Parameters at $t_p=100$ ns, $\langle E_a \rangle=100$ MV/m

T18_vg2.6_disk:



TD18_vg2.4_disk:



Very strong tapering inspired by the idea of having constant P/C along the structure

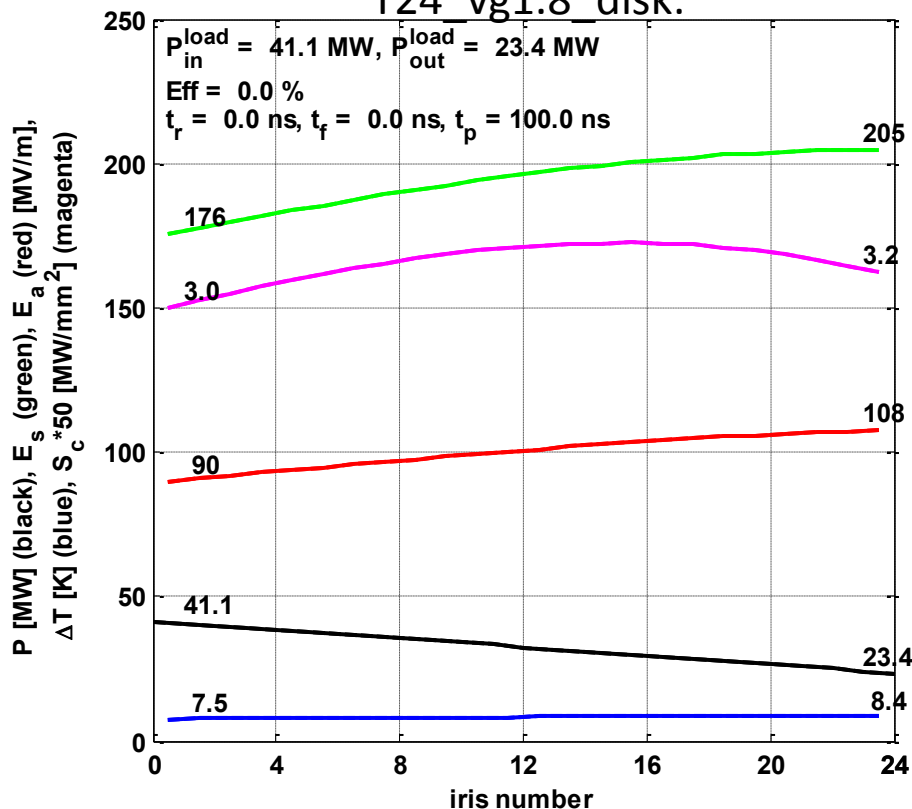
In TD18, all quantities are close to T18 at the same average gradient, except for the pulsed surface heating temperature rise which is factor 5 higher in the last cell.

2nd generation of CLIC X-band test structure prototypes T24/TD24

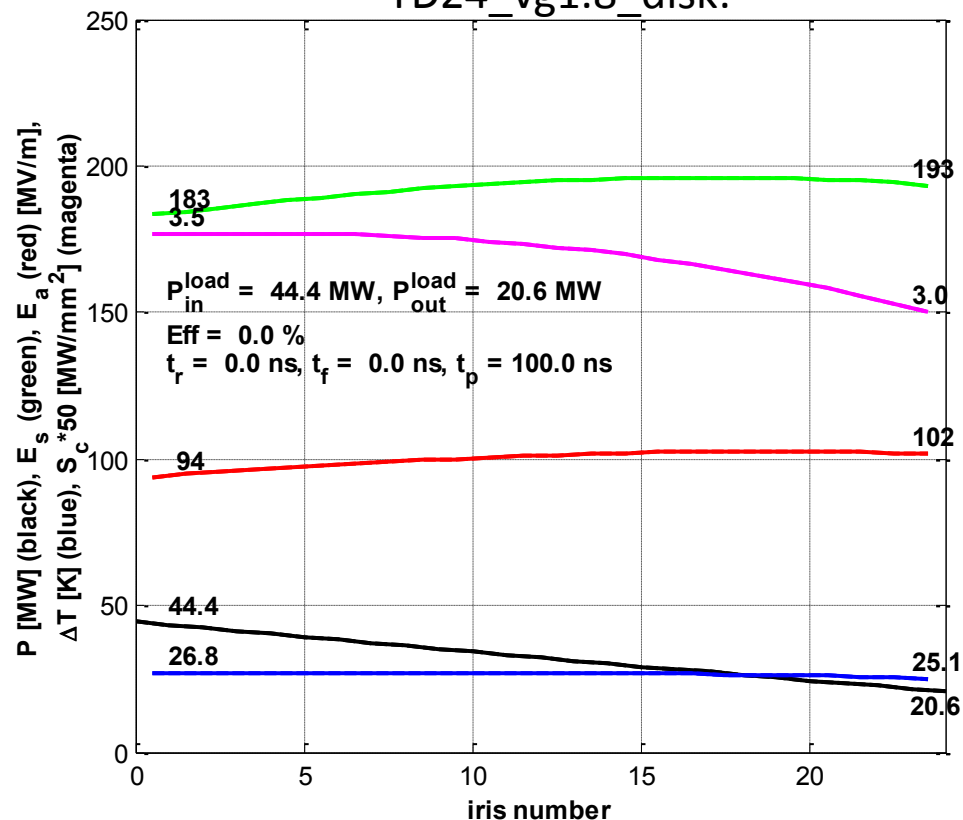
2007

Parameters at $t_p=100$ ns, $\langle E_a \rangle=100$ MV/m

T24_vg1.8_disk:

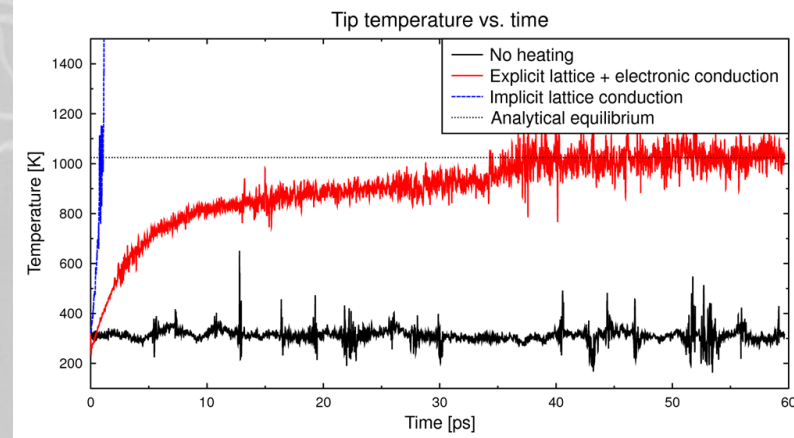
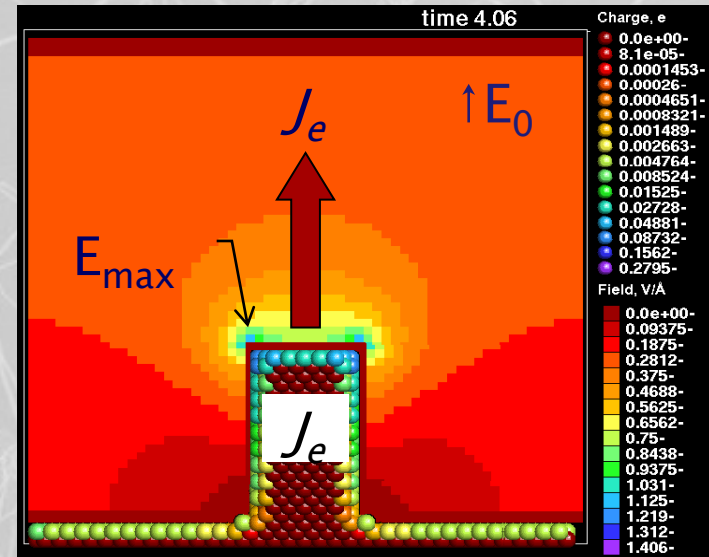
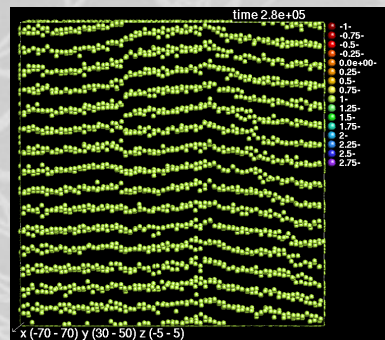
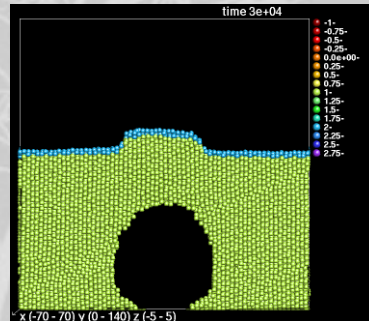
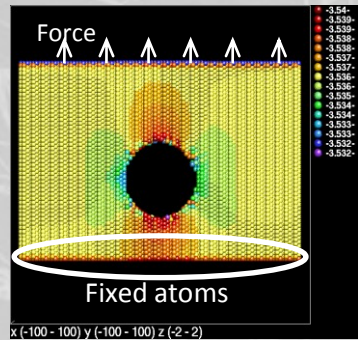
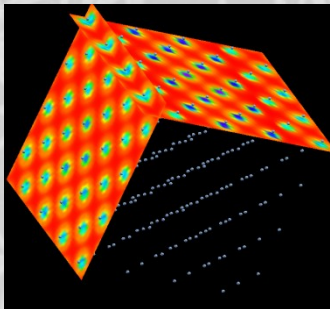
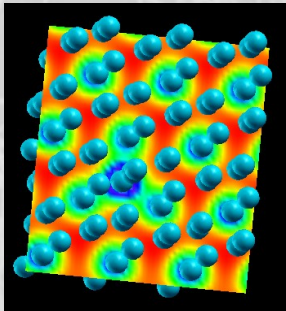
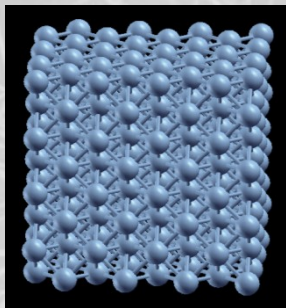


TD24_vg1.8_disk:



Weaker tapering (quasi const gradient) together with smaller aperture (11% instead of 12.8%) reduce surface fields significantly compared to T18/TD18.

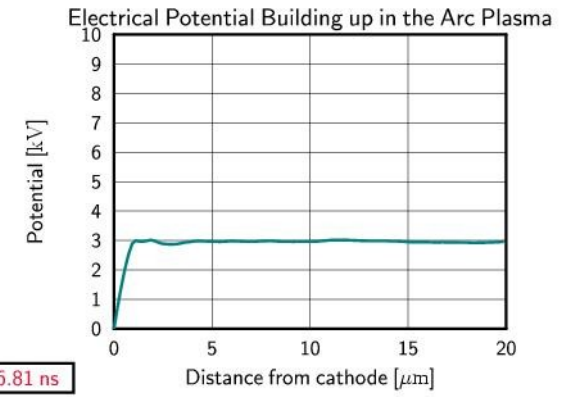
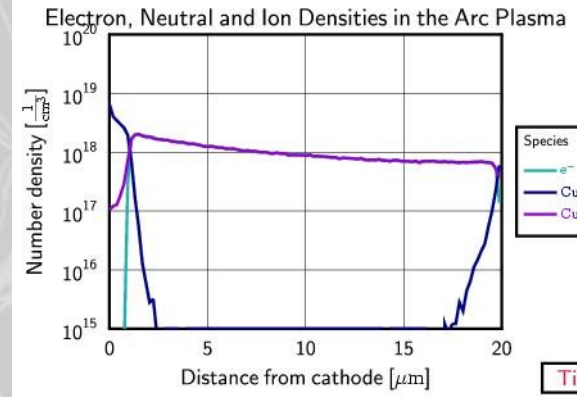
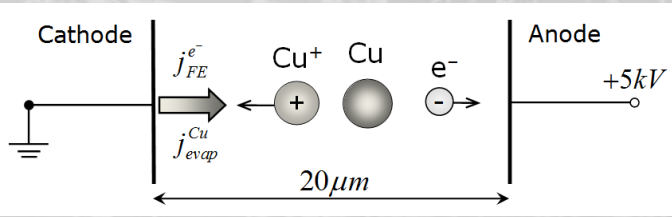
In TD24, all quantities are lower than in TD18 at the same average gradient. In particular pulsed surface heating temperature rise reduced by factor 2.



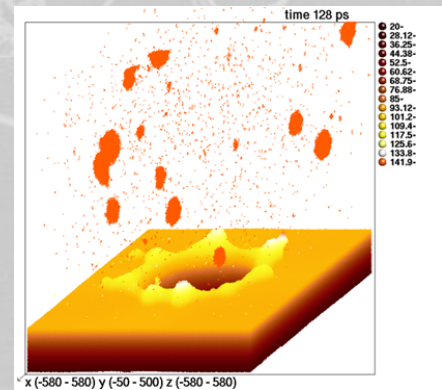
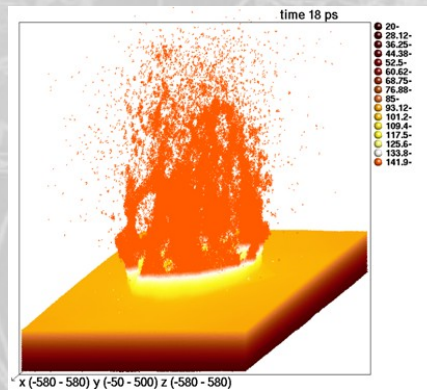
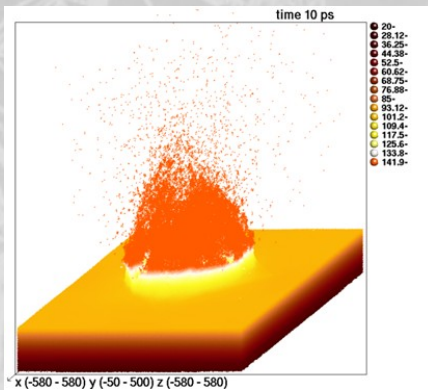
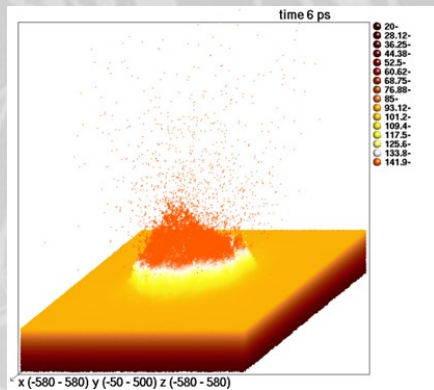
1. Calculation of charge distribution in crystal

2. Emission site formation – breakdown rate

3. Field emission to breakdown trigger, including thermal effects

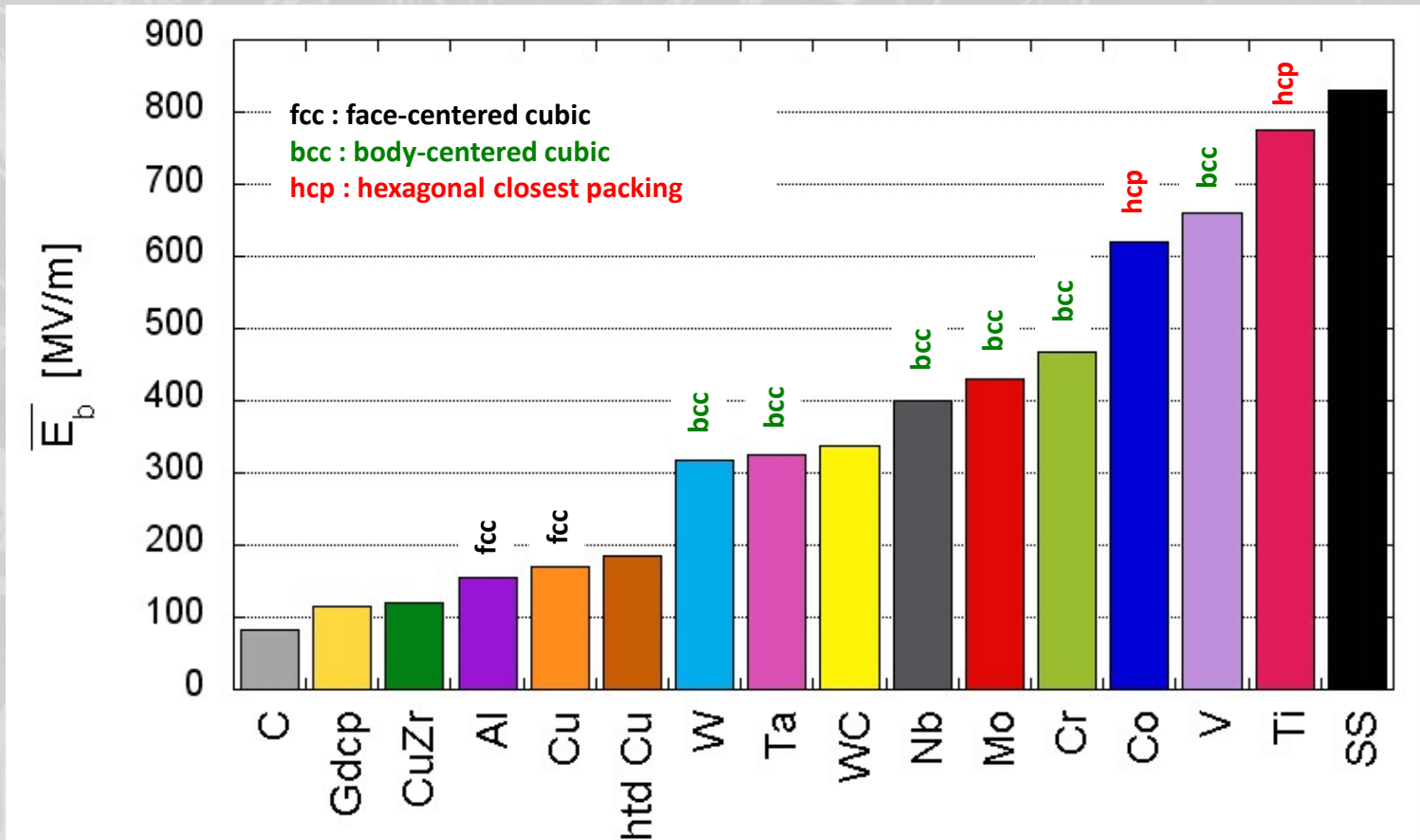


4. Breakdown ignition and plasma formation



5. Surface damage mechanism

Hints for higher performance



Breakdown trigger

Charges collect at cathode non-uniformities under applied electric field [fs, nm]

Structure of surface modified under time/cycles [s, 10^7 pulses, nm]

Field (and thermionic) emission

Structure of surface modified under time/cycles [s, 10^7 pulses, nm]

Tensile electric stress [fs, nm]

Local joule heating [ns, μm]

Thermal stress

Avalanche starts

Field enhanced evaporation of neutrals

(from plasma feeding)

ionization electrons are accelerated away from cathode [mm]

Ionization

Plasma spot forms [few ns, 10-100's of μm]

Plasma dynamics

Plasma sheath forms [μm]

Plasma feeding process

Ions are accelerated towards cathode [μm]

Ions strike cathode and kick out neutrals, ions and electrons

enhanced electron emission due to sheath potential and temperature

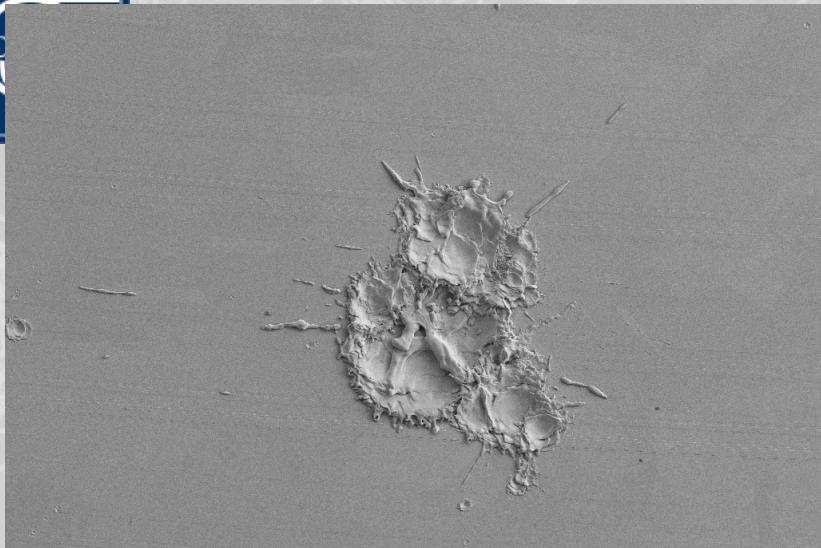
surface melts due to ion bombardment [10-100's of μm]



Electron current accelerated in external field absorbs system energy [mm]

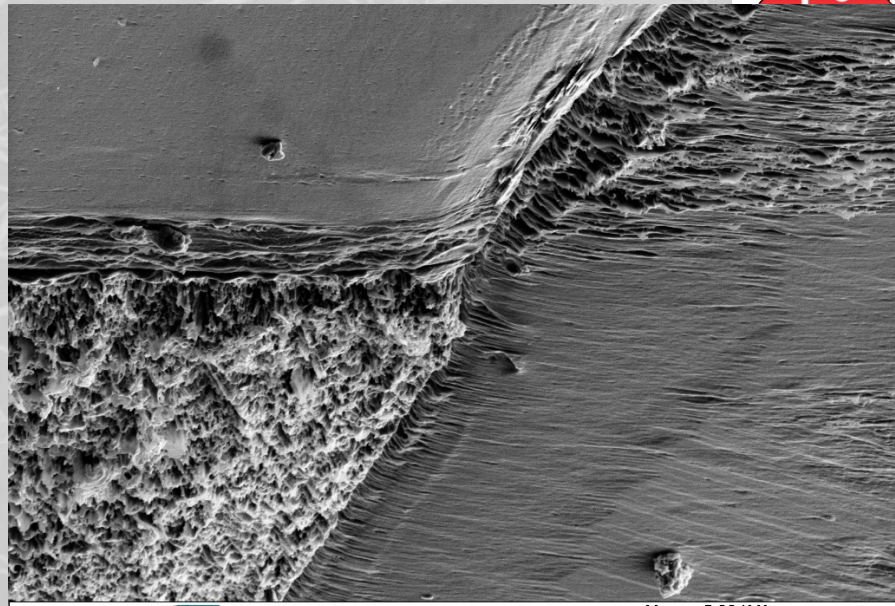
enhanced neutral emission, plasma feeding accelerates

(go to plasma dynamics)

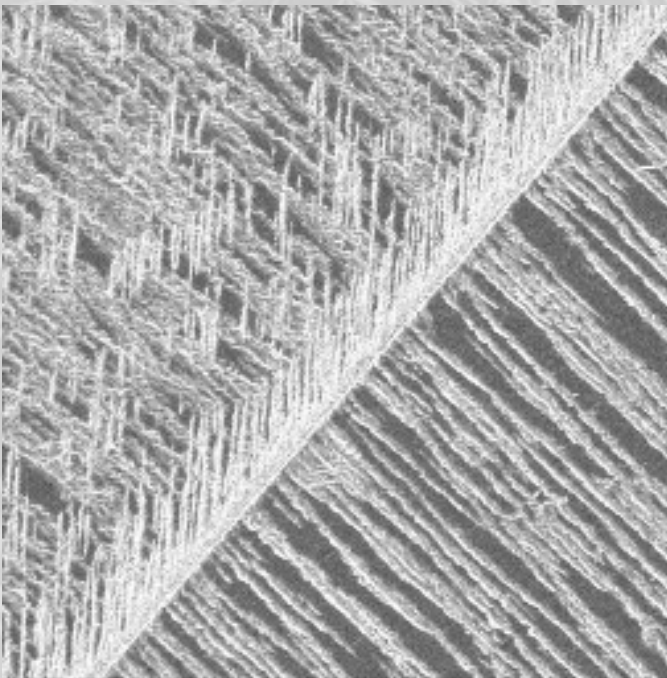
Macroscopic energy transfer



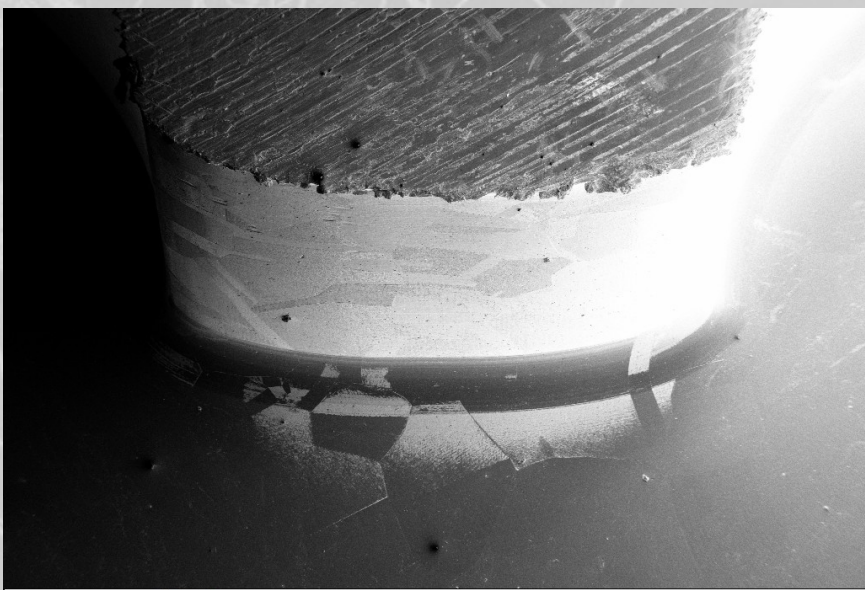
20 μm  EHT = 3.00 kV
WD = 5.1 mm DC-Spark sample Cu(47) Mag = 200 X
Signal A = SE2 Spot 7 (4.65) Markus Aicheler
Date :29 Jul 2010 



1 μm  EHT = 5.00 kV
WD = 25.6 mm TD18 KEK-SLAC Mag = 5.00 K X
Signal A = SE2 Part B Tilt 25° Markus Aicheler
Up-Stream -- NW Date :2 Sep 2010 





460X
Zoom Range: 38x - 960x  10 μm



1 mm  EHT = 5.00 kV
WD = 25.9 mm TD18 KEK-SLAC Mag = 14 X
Signal A = SE2 Part B Tilt 25° Markus Aicheler
Up-Stream -- NW Date :2 Sep 2010 



20 μ m  EHT = 5.00 kV TD18 KEK-SLAC Part C Tilt 30° Mag = 200 X
WD = 15.4 mm Down-Stream -- Cell Wall S-W Markus Aicheler
Signal A = SE2 Stage at R = 135.0° Date :30 Sep 2010 



20 μ m  EHT = 3.00 kV 7N-LG-Cu (45) P. Alknes EN/MME
WD = 5.9 mm Spot #2 Date :24 Mar 2010
Mag = 200 X Signal A = InLens Time :21:53:04 

There is a deep interrelation between achievable accelerating gradient, efficiency, beam dynamics and luminosity through the accelerating structure geometry.

